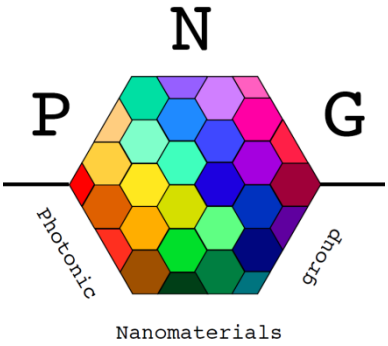

Optical Structures in Diamond

A Materials Science Part II Research Project under the supervision of Dr Jason Smith

Alasdair Morrison

Mansfield College

Trinity Term 2012

1 Abstract

Optical structures are devices that guide and collect light. Optical structures are required in diamond in order to develop and enhance the properties of defect centres found within them. Defect centres in diamond show significant promise for quantum information processing, current research is heavily aimed at the nitrogen vacancy point defect and improving efficiency of coupling light to and from it.

In this project, investigations will be made into defect centres and the processing techniques to develop improved optical structures in diamond. Through the development of an improved microscope set up characterisation of optical structures in diamond that have been both processed in house and externally will be performed. A new system of femtosecond laser milling of diamond will be investigated and its success evaluated, along with processing techniques to use the system for a range of structures.

2 Acknowledgements

This project would not have been possible without the extensive assistance of a number of individuals both within the department and outside. I would firstly like to thank the entirety of the Photonic Nanomaterials Group for their support, guidance and interest, in particular Mr P. Dolan for extensive lab assistance. I would like to thank Professor J. Sykes for regular discussions and help in interpreting results associated with the electrochemical processing.

The invaluable and tireless help of Mr B. Farrington and Dr K. Porfyrakis made possible the cleaning processes and is greatly appreciated.

Mr R. Simmonds and Mr P Salter of the Optical Microscopy Group in Engineering, University of Oxford provided many useful discussions and new samples to examine; as did Dr D. Wildanger of the Department of Nanophotonics and the Max-Planck Institute for Biophysical Chemistry.

Particular gratitude is extended to my supervisor, Dr J. Smith, for his continual assistance and guidance in this project and for his astounding patience.

Table of Contents

3 Introduction

This report will examine the current technology in the field of diamond optics, focusing on the optical structures required to use the large range of diamond defect centres for novel applications.

In the literature survey the current view of the nitrogen vacancy will be presented together with the importance of optical structures for the control of light to develop applications for the defects in diamond. Current processing methods for overcoming the mechanical properties of diamond to realise the optical structures will be explored.

The applications of the research undertaken in this project will be identified in the engineering context section, with the direction that this research aims to help develop.

Within the methodology the characterisation techniques used will be explained, together with the modifications made to the devices to allow specific experiments to be undertaken. The key developments in this area have been the development of a new scanning confocal microscope periscope system; and the use of a novel processing technique in dual aberration corrected femtosecond laser milling. This is followed by an introduction to the samples characterised and the treatments undertaken on them.

The key results will be presented in the results section together with discussions to the importance of the findings identified and comparisons with current literature. This will allow conclusions to be drawn and the further work required to be expanded upon will be suggested.

4 Literature Survey

4.1 Diamond

Diamond is an allotrope of carbon consisting of carbon atoms tetrahedrally bonded to one another by covalent sp^3 bonds. As a material, diamond has a number of remarkable and useful properties [1]. It exhibits extreme hardness (10 on the Mohs' scale) and thermal conductivity (2200 $Wm^{-1}K^{-1}$ in natural diamond, rising to 200,000 $Wm^{-1}K^{-1}$ in ultra-high purity diamond), coupled with low electrical conductivity. The most important properties for optical applications are the high refractive index (2.43 at 500nm) that is constant across visible wavelengths of light [2]; and the large number of optically active defect centres. There are currently in excess of one hundred photoluminescent defect centres [3] with regular discoveries of new centres [4] still being made. The defect centres present the opportunity for development of complex quantum optic systems.

4.2 The Nitrogen Vacancy

4.2.1 Development of Understanding of the Nitrogen Vacancy

The nitrogen vacancy (NV) centre is deemed to be one of the most interesting defect centres in diamond. Clark and Norris identified the vibronic structure of the 1.944eV emission in diamond [5] , publishing the first spectrum of the NV centre in 1971. They proposed that this was the same centre as observed by du Preez in 1965 and formed by the same process of annealing diamond containing isolated nitrogen atoms [6]. It was examined more thoroughly in radiation damaged, high nitrogen impurity diamond [7]. In their study, Davies and Hamer discuss the cause of the NV centre vibronic band; associated with an electron transition between a ground state and an excited state of a centre with trigonal symmetry. They also presented the first evidence that the observed spectra came about from a substitutional nitrogen atom and vacancy pair point defect. The key property of the NV centre is its controllable emission; from the triplet ground state [8] [9] [10] [11] [12], excitation to a higher energy level of an electron by a photon can either return to the ground state by emission of a photon

of wavelength 637nm, or it may fall into a side band [13] [14]. By controlling the spin-state of the ground state, the path the electron takes is controlled. From the S_z=0, the electron will have a 100% probability of emitting a photon, if S_z=±1, 30% of the electrons will fall via the side band and will not emit a photon, and so the state of the defect may be "read" by photon excitation and emission recording. The NV centre shows extremely long spin coherence (in excess of 1 ms), which offers ample opportunity for sophisticated quantum operations [15] [16] [17]. Whilst the exact structure had been under continual deliberation based on models [18] [19] [20] and the previously observed effects, a fully developed and consistent model has now been reached [21]. An additional factor that pushes forward the importance of the NV centre is its stability and lifetime, under optical excitation at room temperature the centres are completely photostable and show no deviance in their emission [22] [15] and are single-photon emitters [23].

4.2.2 Obtaining Nitrogen Vacancy Centres

NV centres may be found in natural diamond; however the presence of other optically active colour centres reduces the usefulness of natural diamond for the majority of applications. Synthetic diamond grown by the high-pressure high-temperature (HPHT) method is used as a primary material in research for its controllable properties; in addition, the scarcity and high price of natural diamond is a severe limit on its use in technological applications. Synthetic diamond still contains a number of naturally formed defects; nitrogen, for one, is introduced from the atmosphere during synthesis [24]. Single-crystal and polycrystal HPHT diamond can be used to observe isolated NV centres. For a more controlled method of obtaining NV centres in diamond ultra-high purity (UHP) diamond is required. UHP diamond can be grown with nitrogen content as low as five parts per billion by chemical vapour deposition [25], or UHP diamonds can be grown through the most rigorous HPHT methods. Implantation of nitrogen atoms is used to generate NV centres when followed by high temperature annealing; in this nitrogen ions are accelerated towards the diamond by a potential difference, they replace carbon atoms in the diamond lattice substitutionally [26]. In order to form an NV centre, the

diamond must be annealed. This allows the diffusion of vacancies to the substitutional nitrogen atoms which reduces the overall strain of the lattice. Native NV centres retain better optical properties over their implanted counterparts [27]. The same technique of implantation can be used for other colour centres; Aharonovich and Prawer report a technique for the implantation of other subsititutional atoms including nickel and chromium; this is achieved by ion implantation followed by further CVD of diamond and annealing [28].

4.3 Optical Structures

4.3.1 Solid Immersion Lenses

In order to utilise the properties of the NV centre, light must be efficiently coupled to it; the high refractive index of diamond in comparison to air leads to large light losses through refraction at the diamond-air interface (see Figure 4-1A). There are a number of simple optical structures that allow for improved light coupling. The most straightforward of this is the solid immersion lens (SIL). The SIL improves light collection efficiency by reducing refraction at surface boundaries, so raising the numerical aperture of the system. Developed by Mansfield and Kino in 1990; it is a hemisphere of high refractive index material, polished to flatness where it is in contact with the material being imaged. The principle of operation is the same as for a liquid immersion lens; the higher refractive index of the SIL replaces the air at the sample interface and gives an improved resolution of $1/n$ where n is the refractive index in the SIL [29]. The hemispherical surface prevents refraction at the surface, as light emitted at the horizontal centre of the hemisphere meets the air interface normal to the surface (see Figure 4-1B). Where the light then meets the SIL-air interface, there is no refraction, this allows more of the light to reach the objective lens, thereby increasing the effective numerical aperture of the system by n, where n is the refractive index of the hemisphere.

4.3.1.1 *Super Solid Immersion Lens*

A second form of SIL exists, this being the super solid immersion lens (sSIL), or Weierstrass Optic. The sSIL operates using the second aplanatic focus of the sphere, that is to say a focal point beyond the centre of the sphere where light arriving at the air-SIL interface is refracted and then focused (see Figure 4-1C).

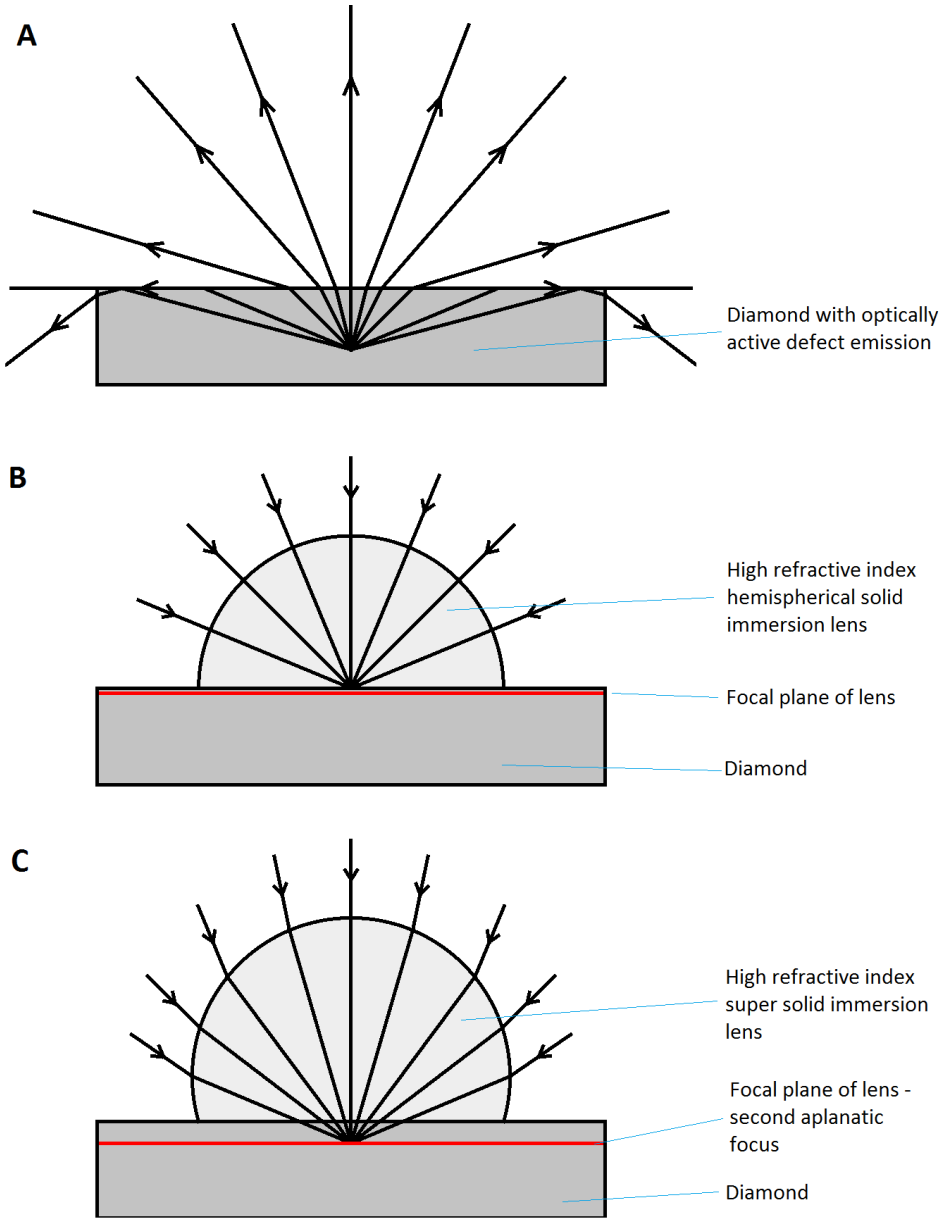

Figure 4-1 – Ray diagrams of the interface between diamond and air (A); and, with the use of a hemispherical SIL (B); and, with the use of a sSIL (C). Images B and C are after Serrels, et al. [30].

A significant advantage of sSIL's is their improvement of resolution by $1/n^2$ with the maximum numerical aperture defined by $1/n_{SIL}$. A further important feature of sSIL's is their magnification increase; this was confirmed to be of the order n^2 by Serrels, et al. using the ray tracing software ASAP of the Breault Research Oganization [30]. This allows for a significant improvement in the light collection and examination of nanophotonic devices, with resolutions reported by Serrels, et al. of the order of 100 nm. One of the primary considerations of the use of sSIL's is the position of the second aplanatic focal point. This is determined by the theory provided by Born and Wolf [31] and is a standard geometric optics problem to give the maximum numerical aperture (NA) for a given focal depth. Given the radius of a sphere as *R*, its refractive index *n*, the depth of the focal plane of interest as *x*, then *D* the required height of the sphere can be determined using:

$$\boldsymbol{D = R\left(1 + \frac{1}{n}\right) - x} \qquad \textbf{Equation 4-1}$$

Barnes, et al. consider the case of the improvement in light collection efficiency using a SIL and a sSIL on a dielectric material with refractive index *n*=3.5 compared with a planar interface using the maximum theoretical calculation efficiency and Monte Carlo simulations to include reflections and refraction at the interfaces. Barnes, et al. show that collection efficiency rises from 3% with a planar interface between the dielectric and air, to 10.4% with a hemispherical SIL of *n*=1.88 and then to 10.8% with a sSIL of *n*=1.88 [32]. It is important to note that this collection efficiency is observed to plateau with rising numerical aperture for the sSIL at an NA of around 0.5; so making it a readily achievable result. The SIL case requires a perfect situation with NA=1 to achieve this efficiency; this is not possible in practice. Zwiller and Björk calculated the collection efficiency of the sSIL to rise to 30% using a material with refractive index, *n* =3.5 [33].

Castelletto, et al. explored the fabrication of SILs directly over an NV centre on the micrometre scale, by modelling with finite difference time domain (FDTD) methods they demonstrated collection efficiencies in excess of 30% could be achieved by placing the SIL in a well with a slightly larger radius than the SIL (see Figure 4-2). Practical results were observed by Hadden, et al. with an NV centre identified in an off-axis position giving a 10-fold increase in light collection [34]. Marseglia, et al.

report a practical method for identifying the position to within 100nm of an NV centre using position markers fabricated in the surface of the diamond, to allow accurate positioning of a SIL on top. This technique demonstrates the SIL operating in excess of 90% of its maximum theoretical collection efficiency [35].

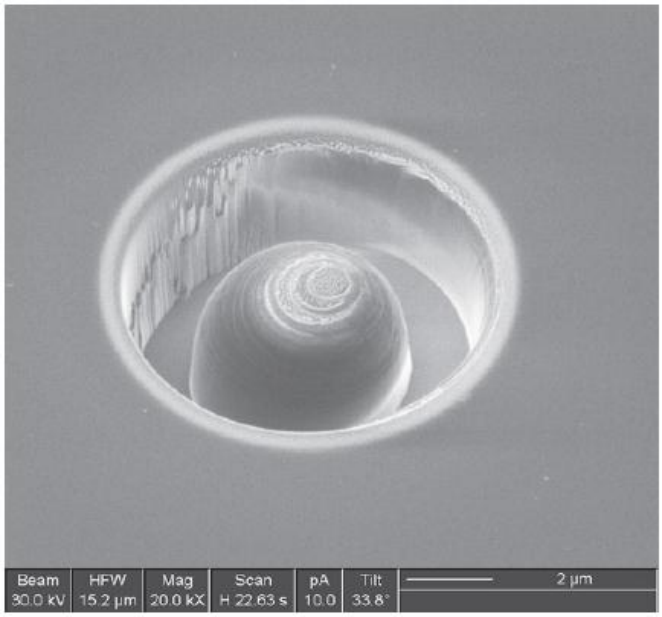

Figure 4-2 – Scanning electron micrograph of a SIL in a well in ultra-pure diamond, taken from Castelleto, et al. [36]

Siyushev, et al. demonstrate the use of a SIL as an off the shelf component to improve collection efficiency by an order of magnitude. They also note that excitation of an NV centre through the SIL gives a smaller excitation volume by an order of magnitude [37]. This may lead to possible improvements in the resolution of stimulated emission depletion microscopy.

4.3.2 Waveguides

With respect to the possible applications of NV centres, the confinement of light within one or more planes is highly desirable in order to be able to direct it in a controlled manner from one point to another. Common demonstrations of the use of waveguides are optical fibres, where light is confined in x and y and allowed to propagate freely in z.

In diamond, waveguides are necessary to route photons from individual NV centres. Olivero, et al. fabricated the first waveguide reported in the literature in high-purity single crystal diamond in

2005 [38]. They formed a tapered waveguide whereby light is coupled into a free-standing channel by tapered edges. As such, the waveguide was multi-mode.

A common technique for diamond waveguides is to create a rib that serves to confine the upper part of a mode, whilst providing sufficient mechanical support from a larger plane structure beneath. Examples that show guided modes include Zhang, et al.'s contribution [39]. Hiscocks, et al. devise a feasible method for bulk diamond processing, utilising photolithography, reactive ion etching and focused ion beams to successfully form a rib that guided a second-order mode [40].

One manner to create a waveguide is to use a material with a different refractive index from diamond either as a substrate for a waveguide, or as the waveguide itself on a diamond substrate. Fu, et al. use this solution to couple NV centres to a gallium phosphide waveguide. This was achieved using photolithography to create a shallow ridge in a GaP layer that was then transferred to the NV centre containing diamond substrate [41]. They recorded large losses in the coupling from defects that arose during processing, and significant losses in the guided modes. However, with improvement this technique shows promise for the easier processing method than that associated with creating waveguides in diamond.

4.3.3 Cavities

There are a large range of microcavity designs that have been employed for confining light. Light is confined by resonant recirculation in small volumes. [42]. An important requirement for NV centre based quantum systems will be the ability to couple light from an NV centre to a cavity.

A number of whispering-gallery microcavities have been demonstrated in the literature. The whispering gallery is a form of cavity where light resonates about the circumference of a disc structure. Liu, et al. couple an NV centre from a diamond nanocrystal positioned in contact with the edge of the gallery into the cavity and then using a tapered fibre, light is coupled into and out of the cavity [43]; they observe strong Rayleigh scattering induced by the nanocrystal; the scattered light couples into a second whispering-gallery microcavity nearby.

Photonic crystal microcavities consist of a regular array of holes in a thin slab of material; an interior defect region consisting of one or more holes of the array left unetched or out of alignment with the array forms the cavity. This gives waveguiding in the direction of the wells and confinement by Bragg reflections in the plane of the array. These cavities are relatively well explored in high refractive semiconductor materials, and also successfully coupled to NV centres [44]. The comparatively low refractive index of diamond as the bulk material presents new design challenges; these were initially faced by Kreuzer, et al. using FDTD modelling [45], they predicted that quality factor (a measure of the performance quality of the cavity; proportional to the confinement time of a photon in the cavity) of the order of 1350 and Purcell factors (a figure of merit for cavities) of the order 90, after taking into account absorption losses. Photonic crystal cavities in single crystal diamond have recently been fabricated by Riedrich-Möller, et al. coupled to a silicon-vacancy centre in the defect region [46]. The qualities of the results are limited by the precision of the cavity construction; a major problem here that is associated with the FIB milling performed, see section 4.4.1.

Microring resonators have been fabricated from diamond using lithographic techniques and dry etching. The work of Faraon, et al. demonstrates an enhancement of the zero-photon line by a factor of 10 [47].

Recently, Hausmann, et al. successfully designed and implemented a nanophotonic network, consisting of a ring resonator coupled to an optical waveguide with grating couplings [48], see Figure 4-3. This ring cavity gives a quality factor of the order of 12000, and coupled with an NV centre situated inside the ring resonator, the total coupling efficiency is given to be around 15%.

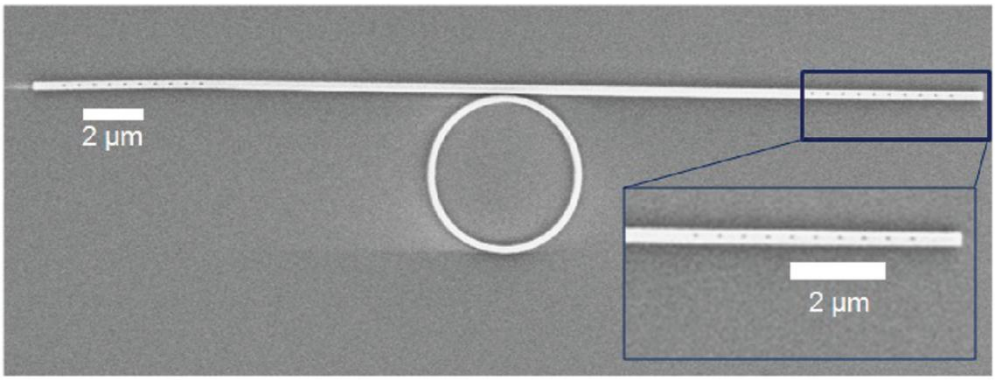

Figure 4-3 – Scanning electron micrograph of a ring resonator coupled to a waveguide with second order gratings on each end – Taken from Hausmann, et al. [48]

4.4 Processing Methods to Obtain Optical Structures in Diamond

4.4.1 Focused Ion Beam Milling

Focused ion beam (FIB) milling is a now commonly used technique for removal of diamond in order to construct optical structures. In this, heavy gallium ions are accelerated toward the target by a potential difference. Electromagnetic lenses control the beam to produce a finely focused spot of the order of nanometres in diameter. The impact of the gallium ions with the diamond surface causes bond damage and eventual ablation of the target material to leave free space. By controlling the beam current, different milling rates can be achieved and nanometer control of the surface roughness is possible [38]. The extreme hardness of diamond presents a number of problems for FIB milling, namely the rate of material removal is extremely slow and significantly reduces the usefulness of the technique as a standalone operation; requiring many hours of expensive equipment use to achieve adequate material removal. As a result, early attempts, such as that by Olivero, et al., made use of helium ion implantation to induce the creation of lattice defects such as vacancies and interstitials, following this, milling with FIB is faster. The damaged diamond must then undergo thermal annealing and chemical etching to produce good surfaces and damage free diamond. Figure 4-2 shows a FIB milled SIL of 2.5µm radius, this was etched using FIB alone but was approximated to give a spherical surface [34]. As can be seen in the image, there are a number of sub-micron scale surface features that will affect light transmission.

One problem arises from the low electrical conductivity of diamond, it must be coated with a thin film of platinum or gold to prevent charge build up and deflection of the beam, however, as the diamond is etched, it creates regions with no conductive pathway, so charge build-up will occur leading to beam deflection [35].

4.4.2 Lithography

Lithographic techniques involve the use of applying a mask and then selectively removing either the areas covered by the mask, or those not covered by the mask.

Inductively coupled plasma (ICP) etching is a relatively recent approach to diamond structure fabrication. It makes use of a high etch selectivity rate between two different materials, in the case described by Zhang, et al. they use a silica substrate to support diamond waveguides that are etched from thin film diamond. Through a photoresist method of photolithography, followed by reactive ion etching they selectively remove regions of diamond to give waveguides [39]

Reactive ion etching (RIE) and ICP have been used to process diamond films to give nanowires, Babinec, et al. successfully produced arrays of nanowires of diameter 200 nm and length 2 µm. The nanowires are smooth walled and successfully guide emission from an on-axis NV centre located in a nanowire [49].

Hydrogen plasma etching of diamond films also shows promise as a controllable graphite removal technique. The technique was investigated by Villalpando, et al. for diamond films on graphite for plasma control in fusion reactors. It was found that the graphite was preferentially etched [50].

4.4.3 Laser milling

Laser milling is an attractive method for material removal in diamond. Unlike materials such as silica, the laser doesn't fully ablate the material through vaporisation, instead the carbon bonds are damaged sufficiently that the carbon loses its structure and becomes amorphous. This technique requires high power femtosecond pulsed lasers that are focused to a diffraction limited spot in the

diamond. Takesada , et al. first demonstrated laser graphitisation of diamond on diamond surface in 2003. Takesada , et al. were able to demonstrate surface milling of the order of 400nm [51]. This process was extended into bulk diamond by Kononenko, et al. who produced simple guide structures at depth [52]. More recently, Simmonds, et al. have designed and implemented a dual aberration corrected system that allows improved resolution of the milled structures and is essential for the controlled generation of micron-scale features [53], the system allows for accurate dimensional control of micron-scale features in depths of material in excess of 200 µm [54] (see Figure 4-4)

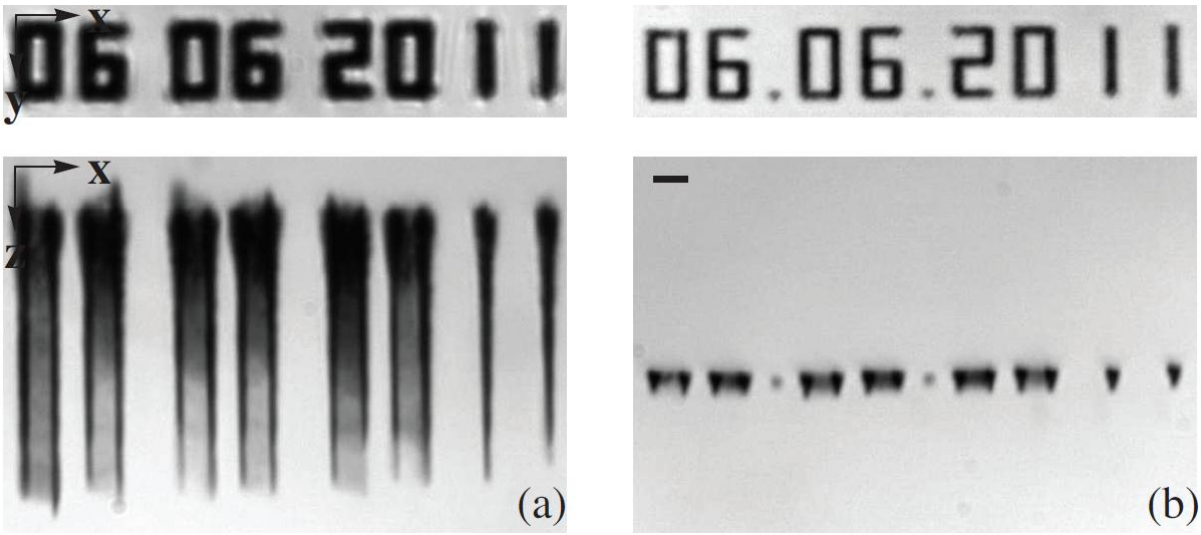

Figure 4-4 – Demonstration of dual-aberration controlled femtosecond laser milling in diamond. Top and side views of the date milled at a depth of 80 µm in bulk diamond, (a) is without aberration correction, (b) is with correction. The scale bar is for a length of 5 µm. Taken from Simmonds, et al. [54].

4.4.4 Graphite removal

A side effect of many of these fabrication processes is the production of graphite or amorphous carbon phases. A number of techniques are proposed in the literature. A commonly used method to selectively remove graphite or organic impurities from the diamond surface is the tri-acid boil of perchloric acid, sulphuric acid and nitric acid. This potentially explosive combination is commonly used to remove material after diamond annealing or for diamond cleaning prior to the application of other techniques [26] [36] [49].

A second technique developed for more aggressive graphite removal is hinted at by Hiscocks, et al., they use a boric acid electrochemical etch [40]. Setting the diamond in a shallow dish of the solution and passing a large current across the diamond set between two electrodes, the graphite – being conductive – carries the current, and so is etched from either end. The diamond is not affected as it does not carry any current due to its high resistivity.

Other areas of science have provided some additional information in to the possibilities of removing graphite from diamond. Carbon is an important electrode material in electrochemistry for its high corrosion resistance [55]. However, carbon may be used as a fuel in high temperature fuel cells, based on solid oxide or molten carbonate technologies (used for their high very high conductivities as solutions) [56]. This was first proposed by Cocks and LaViers in 1994 [57]. Direct conversion of carbon fuels is by oxidation to CO_2 however the process is highly rate dependent of the surface area of the graphite [58]. One side effect of this process is that for the graphite to be removed, it is often necessary to heat the material in excess of 700°C – an area where the diamond may start to become unstable [59], [60]. One possibility is the use of ionic liquids as the electrolyte – these are low melting temperature ionic solids that have exceptional conductivities – at temperatures below 100°C [61], [62].

5 Engineering Context

Optical structures in diamond are essential to realise the potential of the defect centres present in diamond. The NV centre is a unique defect that has many potential applications, ranging from quantum information processing through to biological labelling. Quantum information processing is deemed as one particularly interesting area for the NV centre [63], however much of the current research faces difficulty in the ability to couple light to and from defect centres efficiently [64] and the ability to maintain low loss systems. Added to this are the extreme mechanical properties of diamond that can lead to extensive difficulties in processing [1] [60].

Despite these shortcomings of diamond, it remains an attractive material due to the potential for creating diamond chip systems using nanophotonic devices [65]. As NV centres are single-photon sources, they are strong contenders for optical quantum computing applications [66] and quantum cryptography [67]. This is assisted by the ability to entangle quantum states with millisecond stability with the potential to exceed tripartite entanglement [16]. This may help to create quantum networks where interactions between NV centres or other point defects [68].

The low thermal expansion coefficient of diamond, coupled with its high thermal conductivity makes it an attractive material for classical optics devices such as low temperature lenses. The limitations to current implementation are the difficulties in processing, as stated above.

Diamond also sees significant application in biotechnology due to its complete biocompatibility [69]; the use of nanodiamond (nanometre diameter diamond particles) as a fluorescent marker being one key area of interest.

6 Methodology

6.1 The Scanning Confocal Microscope

The scanning confocal microscope (SCM) is an optical microscope that is an inherently useful tool for high resolution imaging of transparent crystals and subsequent experimental investigations. It operates using a laser to excite optically active structures within, or on the surface, of a sample. The emission of light is detected using a single-photon avalanche detector (SPAD). Through the use of an electronically controlled scanning mirror, the excitation beam can be scanned in the x and y plane of the sample, focus is kept using telecentric lenses and an image can be constructed from a raster patterned scan. The scanning confocal microscope used in this project is that designed and built in house by Grazioso, Patton and Smith [70], with some modifications.

6.1.1 Optics of the Scanning Confocal Microscope

6.1.1.1 Excitation Optics

Light of 532nm is emitted from a continuous wave laser of 200mW. It passes through an attenuating filter and is then coupled into a single-mode fibre optic cable. It then enters the scanning unit through a collimating lens; this forces the refracted light that leaves the fibre optic cable to return to collimation (i.e. parallel wavefronts). The beam is then reflected by a dichroic mirror (a mirror that only reflects certain wavelengths of light – in this case wavelengths shorter than 550 nm) on to the scanning mirror, which reflects the light through the telecentric lenses, and so onto the objective lens where it is focused to a fine point on the sample.

6.1.1.2 The Telecentric Lenses

An important aspect of the functioning of the scanning confocal microscope, and that which allows the scanning to take place, are a pair of telecentric lenses. The telecentric lens as an individual focuses light to infinity on one side (i.e. a collimated beam) and to a set focal distance on the other

side. By arranging two telecentric lenses together, the effect of the angle that the beam enters the first telecentric lens is replicated at the second (see Figure 6-1). This ensures that the beam axis always enters the objective at the centre of the lens; giving a subsequent increase in the field of view of the objective lens, limited by the diameter of the telecentric lenses and not the objective. By using two telecentric lenses instead of one (which would allow a similar effect) the magnification of the lenses cancels; and the spherical aberrations of the two lenses sum to zero.

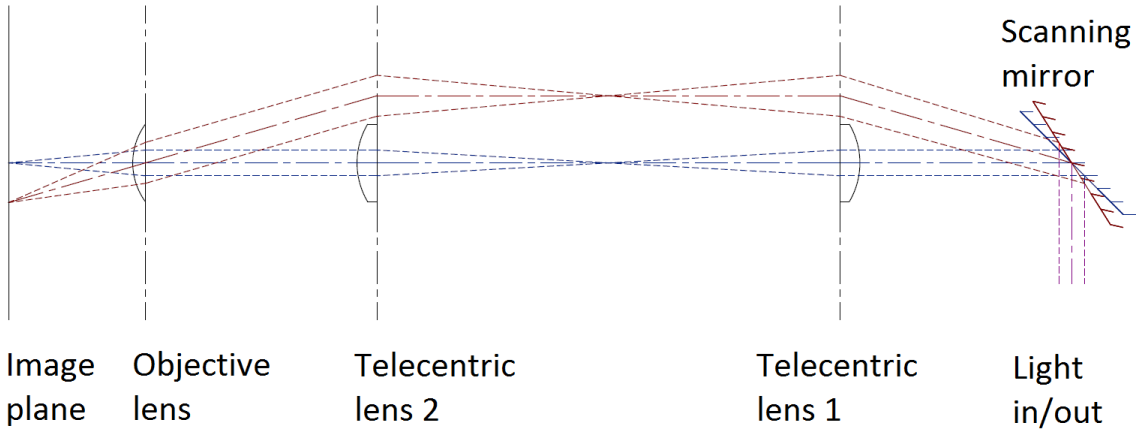

Figure 6-1 – Telecentric lens operation

6.1.1.3 Collection Optics

Light reflected or emitted from the sample is collected via the objective lens and then follows the same optical axes as the excitation optics. After it is reflected by the scanning mirror, it passes through a dichroic mirror, without reflection, followed by a notch filter to block reflected excitation light. It then enters a focusing lens which couples it into a fibre-optic cable which is coupled to the SPAD. This emits an electrical signal each time a photon is detected, up to a maximum collection rate of around 10 MHz. The data is recorded by a computer and the total photon counts for a given dwell time at each position on the scan are recorded to build a map of photoluminescence intensity.

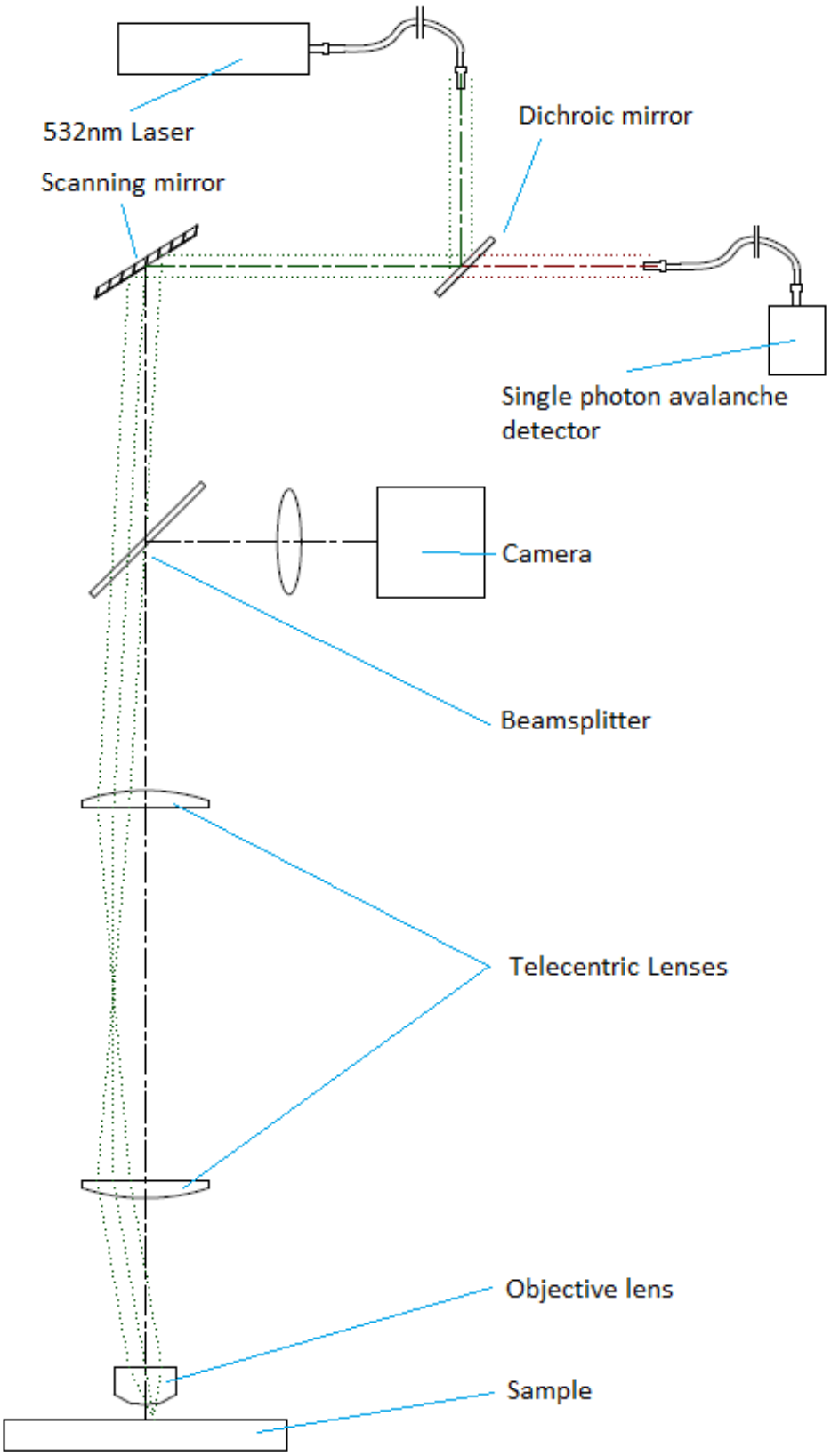

Figure 6-2 – Schematic drawing of scanning confocal microscope, after drawings from Grazioso, et al. [70]

6.1.2 Adjustments made to the Scanning Confocal Microscope

The SCM was designed to be used on a horizontal optics bench. As such, the sample must be mounted perpendicular to the optical axes, so it lies perpendicular to the bench, in the vertical plane. This forces the sample to be fixed to a sample mount by some adhesive, usually nail varnish or silver dag (the latter preferentially; for its minimal photoluminescence and to make a thermal contact). When operating with thin films it is preferential to mount them on the horizontal due to the difficulties in cleaning the samples of the adhesive after mounting. Solid immersion lenses can only be mounted horizontally as the use of any adhesive greatly reduces their effectiveness. As such, a compact bench mounted device was designed to allow for horizontal sample mounting for imaging.

The primary objective in the design was to have a system that moved all the optical axes from the horizontal to the vertical. The immediate solution is to move the scanning head unit into a vertical position, but owing to the focal length of the telecentric lenses this creates a large free-standing structure that becomes highly sensitive to vibrations and movement. It was identified that a series of mirrors could be used to adjust the optical axes. This led to the construction of a fixed periscope that allows different sample mounting modules to be used (see Figure 6-3). Including different size objective lenses, a cryostat for cooling the sample to liquid nitrogen temperatures on the bench (see Figure 6-5) and to allow initial examinations with other setups used within the group.

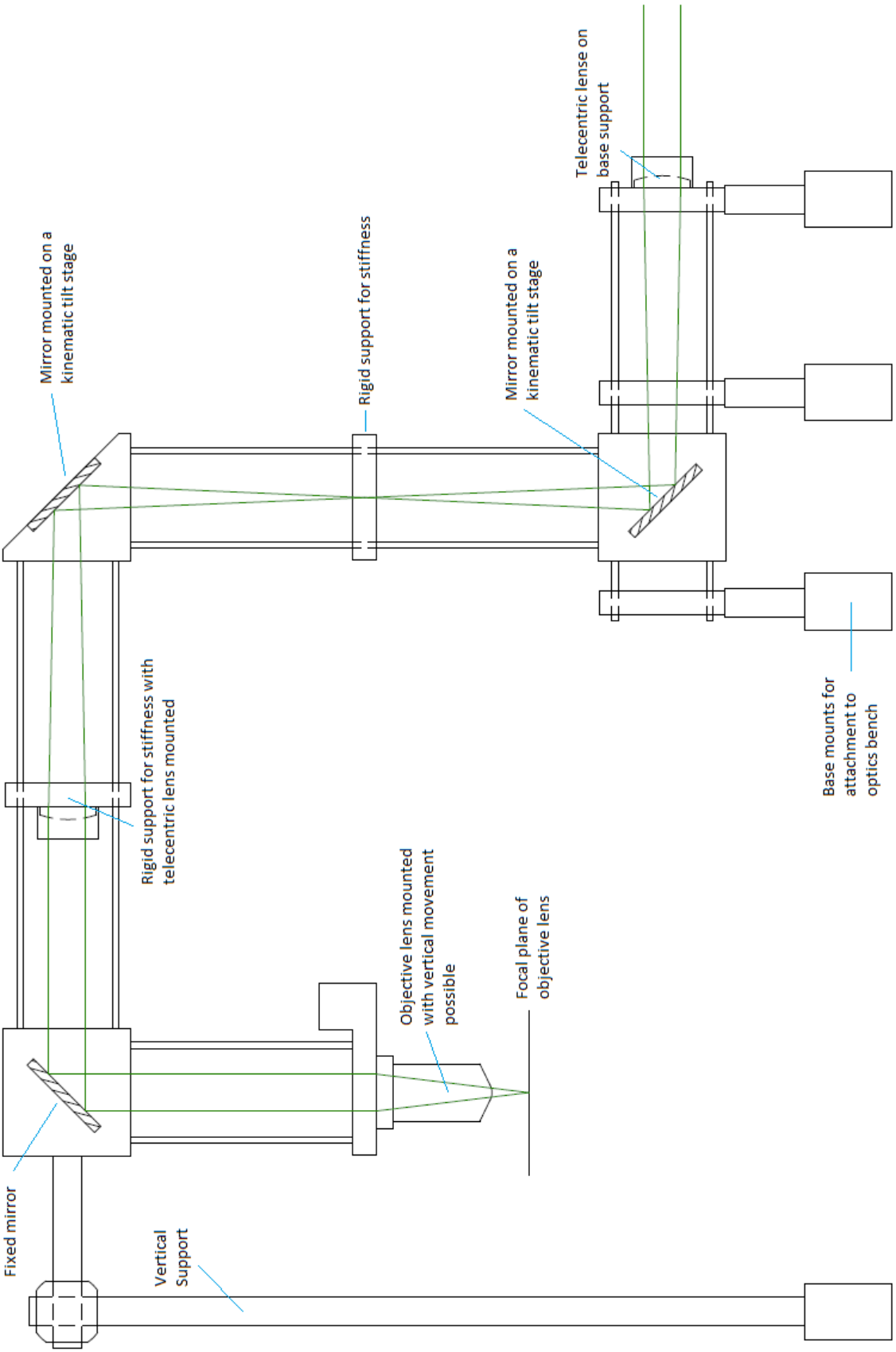

Figure 6-3 – Schematic drawing of scanning confocal microscope periscope design

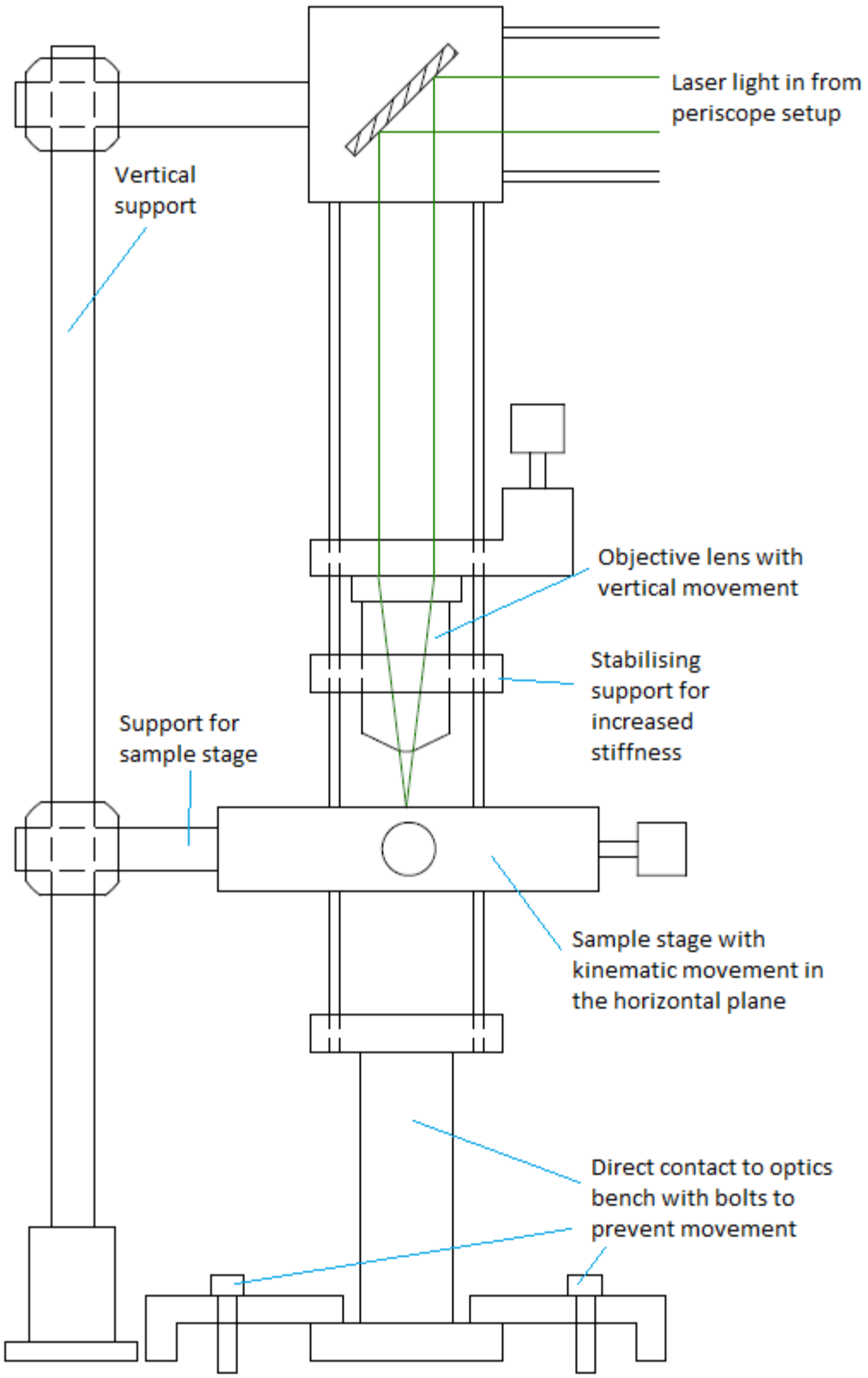

Figure 6-4 – Schematic drawing of high stability setup for sample imaging in the periscope system of the scanning confocal microscope

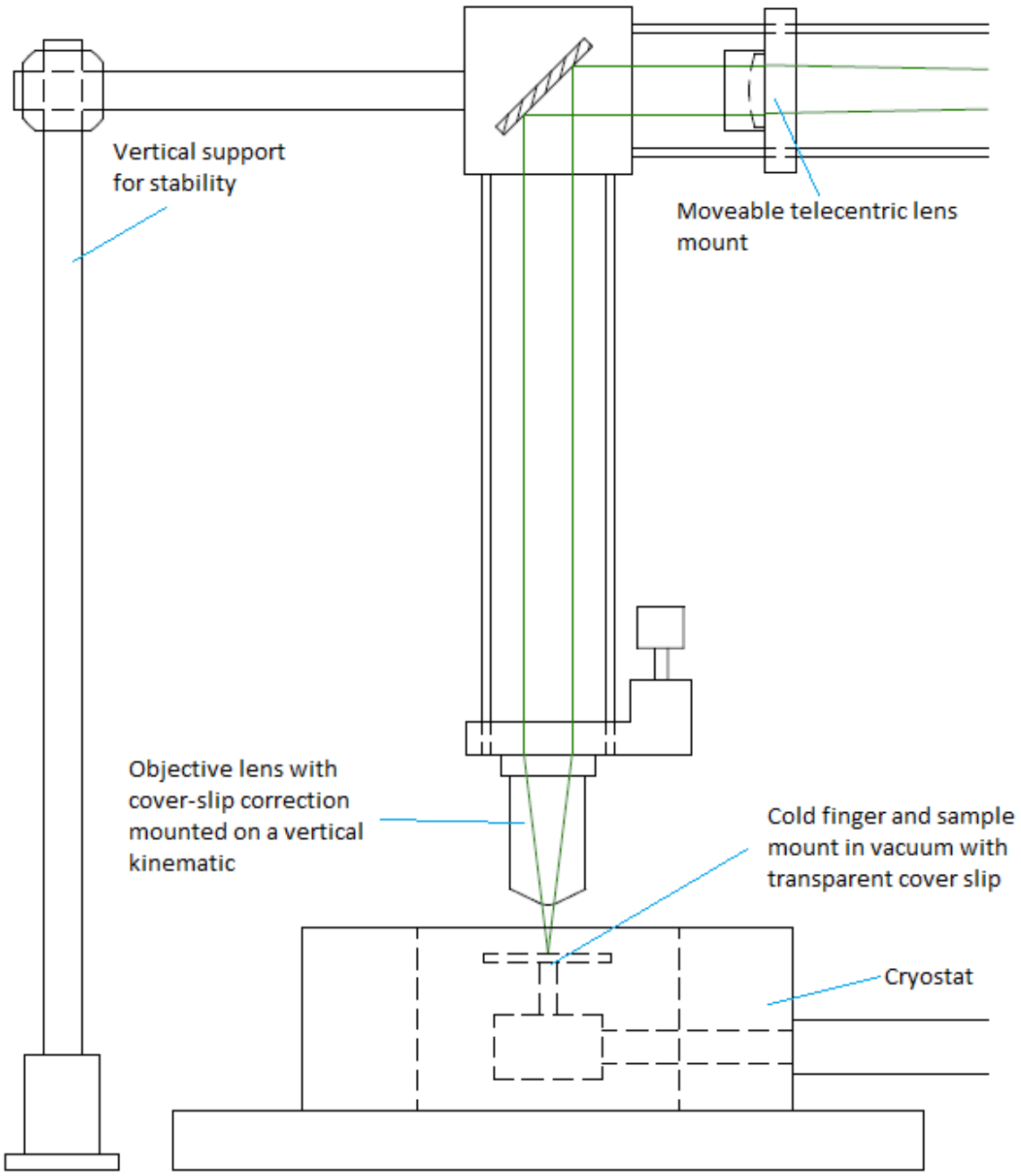

Figure 6-5 – Schematic drawing of setup for imaging at liquid nitrogen temperatures using a cryostat in the periscope system of the scanning confocal microscope setup

The periscope was designed primarily for simple photoluminescence experiments where the sample is illuminated and imaged from above. The primary consideration of the periscope design was maintaining alignment of the beam to the optical axis. This was achieved by fixing the x and y alignment of the objective lens and aligning the beam by tiltable mirrors to the centre of the objective lens. In order to have complete freedom of alignment, only two of the mirrors need to be tiltable, it was decided that fixing the final mirror (i.e. the one closest to the objective lens) would give the best stability. This is because the other two mirrors are situated between the two telecentric lenses, where the beam is less sensitive to movement. However, a key requirement of the design of the mirror system was to ensure that none of the mirrors were located close to the focal point of the telecentric lenses where fluorescence from dust particles would give a strong background signal.

Stability of the periscope is maintained using the cage system of interconnected rods and machined cubes. The sample is securely fixed to the mount which is in turn connected directly to the objective lens mount and the bench (see Figure 6-4). This is of particular importance to maintain alignment of the microscope as thermal drift occurs due to differential heating rates of the microscope construction components. These are readily caused by small thermal gradients in the vicinity of the SCM.

6.1.3 Experimental use of the Scanning Confocal Microscope

6.1.3.1 Objective lens Choice

When using the SCM, it is necessary to determine which objective lens should be used for the particular sample under examination. It is not yet possible to change the lens whilst retaining the same position on the sample.

The primary lenses used are:

10x - NA 0.4 – Large imaging area, but low resolution, not sufficient to image individual defect centres

20x - NA 0.4 – Large imaging area, low resolution, insufficient resolving power to observe individual defect centres

50x - NA 0.45 – Bausch and Lomb – Long working distance lens (in excess of 15mm), allows for the examination of samples using the solid immersion lenses.

100x - NA 0.9 – Olympus Mplan – High magnification lens for observation of single defect centres, a spot size smaller than 300nm achievable with 532nm laser (by Abbe diffraction limitations)

6.1.3.2 Sample preparation

Diamond samples are prepared according to the requirements of the setup. Typically, a mounting block was chosen for its lack of photoluminescence, with polished aluminium blocks used for the larger diamonds and fused silica blocks for smaller pieces of diamond.

Before examination, the diamond surfaces were cleaned using a methanol wipe, followed by a deionised water rinse and then an acetone wipe. The diamond was then fixed to the surface of the chosen mounting block using silver dag to prevent thermal drift during examination; this was then attached to a lens tube cap (a thin aluminium cylinder with a thread to allow secure fixing to the SCM) and secured to the sample stage.

Where the SILs are to be used, further preparation is required to ensure good surface contact between the SIL and diamond and to reduce the interface effects of refraction and reflection. To do this, a small drop of oil immersion liquid (n=1.5) was applied to the diamond surface, any excess removed at this point by absorption into a lens tissue. The SIL or sSIL was then placed on the oil film and vertical pressure applied. Any further excess oil was removed and the sample examined (see Figure 6-6).

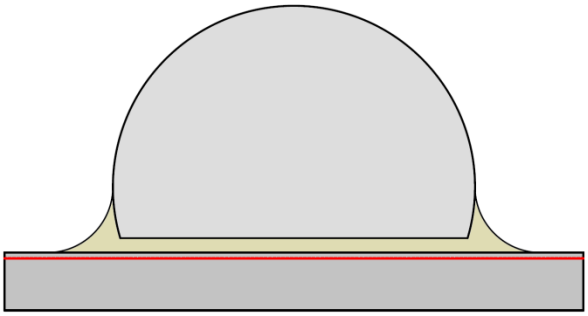

Figure 6-6 – A super solid immersion lens on top of diamond with a high refractive index oil film between

6.2 Spectrograph

Spectra were obtained from the sample by coupling light from the collection optics to an Acton Research Corporation Spectapro 2500i monochromator/spectrograph. The spectrograph operates by diffracting the light and measuring the intensity at different wavelengths across a charge-coupled device (CCD) imaging sensor. The light passes through a 550nm long pass filter before entering the spectrograph.

6.3 Hanbury-Brown and Twiss measurements

Hanbury-Brown and Twiss (HBT) measurements were obtained using a beamsplitter on the SCM collection fibre. Two single-photon avalanche detectors were used to obtain electrical signals for the detection of photons and the electrical signals were fed into an Edinburgh Instruments T900 time-correlated single photon counter. This was calibrated using the output of a pulsed laser driver set at constant frequency in the MHz range.

6.4 Acid Boils

It is found that the surface of diamond has a high affinity for organic contaminants and other impurities. It was regularly observed that diamonds gathered surface contaminants during their examinations. As a result these materials must be removed to allow imaging to take place. This removal is achieved through the use of acid boils and soaks, presented below in order of increasing severity.

6.4.1 Nitric Acid Soak

Soaking the diamond samples in nitric acid at 69% concentration for time periods in excess of 24 hours removes a large proportion of organic impurities.

6.4.2 Aqua Regia Soaks and Boils

Aqua regia is a strong acid solution formed by combining hydrochloric acid and nitric acid at the strongest concentrations available in the ratio of 3:1 respectively. This was found to be much more strongly oxidising than the nitric acid and was as such used for reflux boils as well as longer soaks.

Increasing the temperature through boiling provides additional activation energy for the oxidation of organic materials on the diamond surface, reflux apparatus was used to prevent significant loss of acid during the reaction, although a large volume of chlorine was lost during each run.

6.4.3 Tri-Acid Boils

In cases where the aqua regia solution was found to be insufficiently oxidising to remove impurities, a stronger tri-acid boil has been devised; the tri-acid solution being a mixture of perchloric acid, sulphuric acid and nitric acid. All three acids are to be used at the highest concentrations available, in this case 70%, 92% and 69% respectively. The perchloric acid and nitric acid are strong oxidising agents; sulphuric acid is added to increase the concentration of the other acids by dehydration to give anhydrous acid conditions.

All samples that are to be subjected to the tri-acid boil are to be first soaked overnight in nitric acid to remove any remaining organic material. Following the acid boil, the samples will be rinsed in an excess of de-ionized water and then dried in lens tissue.

6.5 Samples

A number of samples where characterised in this study. Explicit details are below.

6.5.1 Engineering Diamond 1 – "ED1"

ED1 is a high purity diamond from Element6. It is a plasma enhanced chemical vapour deposition (PECVD) grown diamond of dimensions 3.9 mm × 3.9 mm × 0.5 mm. A number of processes have been applied to it. Initially a number of test structures were milled (see Figure 6-7) using the dual aberration corrected femtosecond Ti:Sapphire laser (see section 4.4.3) by Richard Simmonds of Dr Martin Booth's group.

ED1 was then annealed at 1100°C for 1 hour in vacuum of at least 1×10^{-5} atmospheres. Following this the sample was cleaned in an aqua regia boil for 1 hour. After each stage the diamond and features were imaged using scanning confocal microscopy and their spectra recorded.

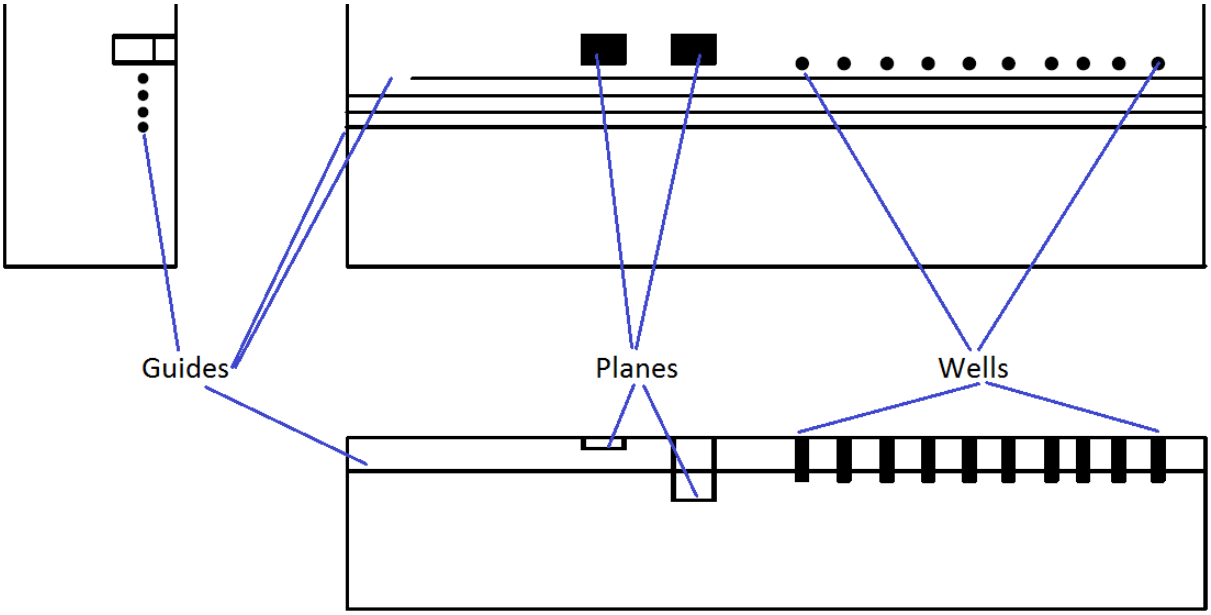

Figure 6-7 – Schematic drawing of graphitic test structures milled in diamond ED1, including planes, guides and wells

6.5.2 Engineering Diamond 2 – "ED2"

ED2 is a high purity diamond bought from Element6. It is a PECVD grown diamond of dimensions 3.9 mm × 3.9 mm × 0.5 mm. It was imaged using scanning confocal microscopy and then, as with ED1, milled with a number of structures using the dual aberration corrected femtosecond Ti:Sapphire

laser (as above), the structures were milled following characterisation of the structures in ED1. A series of waveguides and a capacitor-like device were constructed (see Figure 6-8). The structures were characterised using optical microscopy (in transmission mode) and then annealed at 1100°C for 1 hour in vacuum of at least 1×10^{-5} atmospheres. The sample was then soaked in aqua regia for 48 hours and then boiled with a fresh solution for 2 hours. The effects of which were documented using optical microscopy.

6.5.3 Single Crystal 10µm film – "SCTF"

Originally a single crystal thin film of dimensions 3mm by 3mm by 0.01mm; the sample was obtained as small crystals of various sizes. A small segment was subject to nitrogen-implantation by Dr Dominik Wildanger of the Department of Nanophotonics and the Max-Planck Institute for Biophysical Chemistry. The segment measured approximately 0.2 mm by 1.75 mm and was examined before and after processing. Nitrogen implantation was carried out by accelerating nitrogen ions through a hollowed scanning tip of an atomic force microscope [26]. The returned sample was then annealed resting on a fused silica block at 800°C for two hours under a vacuum in excess of 1×10^{-5}atm. The sample was boiled for two hours in a concentrated aqua regia solution at 100°C to remove surface contaminants.

The sample was imaged with the SCM whilst resting on a fused silica block before and after annealing. It was additionally imaged using optical microscopy.

6.5.4 Polycrystal 5µm film – "PCTF"

A polycrystal diamond film measuring 15mm by 15mm by 0.005mm was provided by D. Wildanger and S. Hall of the University of Göttingen. The thin film was mounted on an aluminium block by depositing on an acetone film using a scalpel blade. The evaporation of the acetone leaves the film held in place by Van der Waals forces. Removal from the block caused fracture of the diamond, leaving a number of different sized pieces. The smaller pieces were mounted on a fused silica block using silver dag for examination.

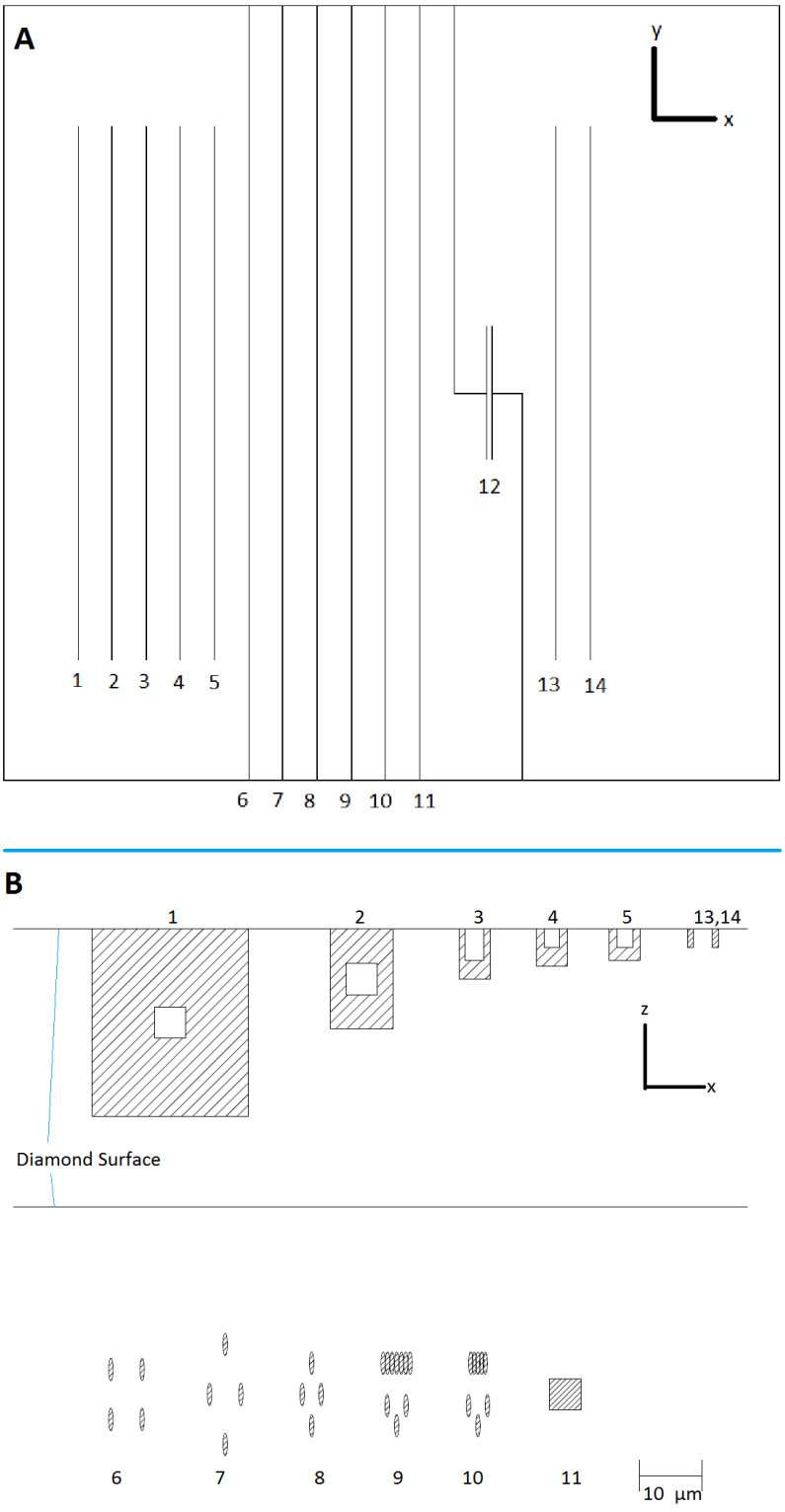

Figure 6-8 – Schematic drawing of laser milled structures in ED2. Hatched areas are damaged diamond structures. In A, all guides are 100 µm apart – structure 12 is a plate capacitor-like structure. B shows cross section of all structures to scale and appropriate depth below diamond surface.

6.5.5 Polycrystalline Diamond Slab – "PCDS"

A polycrystalline diamond of dimensions 10mm x 10mm x 0.5mm was obtained from Element6. No further details are available as to its processing. It was characterised using the scanning confocal microscope.

6.5.6 Diamond Solid Immersion Lens – "SIL1"

A diamond solid immersion lens manufactured by Element6, with diameter of 1.5 mm, with a refractive index of 2.4.

6.5.7 Cubic Zirconia Solid Immersion Lens – "SIL2"

A cubic zirconia hemispherical solid immersion lens of diameter 2.2 mm, with a refractive index of 2.0.

6.5.8 Cubic Zirconia Super-Solid Immersion Lens – "sSIL"

A cubic zirconia super solid immersion lens or weierstrass lens of radius 0.9 mm was obtained, the lens has a depth of 1.34 mm (measured by vernier calipers), so by equation 3.1 the focal plane of the sSIL is at a depth of 10 µm. The sSIL has a refractive index of 2.0 and is cleaned before use using ultrasonic excitation in acetone.

6.6 Efficiency of the Optical System

The light collection efficiency from a single defect emitter in diamond may be calculated using the solid angle integral and details of the objective lens system.

6.6.1 Emission Efficiency

Considering the case of a single emitter sitting in some plane below the diamond surface; the light that reaches the diamond surface at an angle smaller than the critical angle, θ_c for total internal reflection will be emitted from the diamond.

$$\theta_c = \theta_t = \theta_t$$

$$\theta_c = \arcsin\left(\frac{n_2}{n_1}\right)$$

Calculating the fraction of light of the total emitted that passes through a cone of angle $\theta < \theta_c$, using the solid angle integral for Ω, where Ω is the solid angle measure in steradians from a total solid angle of 4π for a sphere.

In spherical polar coordinates

$$\Omega = \sin(\theta)\, d\phi d\theta$$

$$\Omega = \int_0^{\theta_c} \int_0^{2\pi} \sin(\theta)\, d\phi d\theta$$

$$\Omega = 2\pi \int_0^{\theta_c} \sin(\theta)\, d\theta$$

$$\Omega = 2\pi(1 - \cos(\theta_c))$$

The emission efficiency is thus given by; $\Omega/4\pi$. This is 4.55% for the case of emission through a planar air-diamond interface.

6.6.2 Collection Efficiency

To examine the collection efficiencies, the numerical aperture (NA), of the lens must be taken into account. As $NA_{lens} = nsin(\alpha)$, where α is the half angle of the maximum cone of light that can enter the lens, so the critical angle for the light to be collected - taking into account the objective lens - becomes:

$$\theta_c = \arcsin\left(\frac{NA_{lens}}{n_1}\right)$$

For the case of the planar air-diamond interface (see Figure 4-1A) the collection efficiency, η, with the air objective above is thus given by:

$$\eta = \frac{1 - \cos\left(arcsin\left(\frac{NA_{lens}}{n_1}\right)\right)}{2}$$

Where the hemispherical SIL's (h-SIL) have been used (see Figure 4-1B), we expect to see a significant increase in the emission efficiency, but equally, a decrease in the numerical aperture of

the lens as a long working distance (LWD) lens is required to accommodate the macro SIL's of the dimensions given in sections 6.5.6 - 6.5.8.

The effective NA of the system is controlled by the refractive index of the SIL material:

$$NA_{eff} = NA_{lens} n_{SIL}$$

$$\eta_{h-SIL} = \frac{1 - \cos\left(arcsin\left(\frac{NA_{lens} n_{SIL}}{n_1}\right)\right)}{2}$$

In the case, where a super solid immersion lens (sSIL) is used (see Figure 4-1C), the effective NA is controlled by the square of the refractive index:

$$NA_{eff} = NA_{lens} {n_{SIL}}^2 \qquad \text{until,} \quad NA_{eff} = n_{SIL}$$

$$\eta_{sSIL} = \frac{1 - \cos\left(arcsin\left(\frac{NA_{lens} {n_{SIL}}^2}{n_1}\right)\right)}{2}$$

Table 6-1 shows a comparison of the results of the above calculations for the theoretical maximum collection efficiencies. In all the cases, collection is for the perfect case, for example; the h-SIL would have a point defect emitting at the interface of the SIL and the host material, centred exactly in the centre of the SIL.

Setup	Lens	η
Planar interface between air (n=1) and diamond (n=2.4)	100x Air, NA = 0.9	3.65%
Planar interface between oil (n=1.5) and diamond (n=2.4)	100x Oil Immersion, NA = 1.25	7.31%
Diamond (n=2.4) with cubic zirconia h-SIL (n=2.0)	50x LWD, NA = 0.45	3.65%
Diamond (n=2.4) with diamond h-SIL (n=2.4)	50x LWD, NA = 0.45	5.35%
Diamond (n=2.4) with cubic zirconia sSIL (n=2.0)	50x LWD, NA = 0.45	16.9%

Table 6-1 – Comparison of calculated collection efficiencies for the various setups tested (note – an oil immersion lens was also not used – it's collection efficiency is included for completeness).

It must be noted that the effectiveness of the hemispherical SIL is severely limited by the numerical aperture of the objective lens. This could be improved by the use of either a lens with a higher numerical aperture but still retaining a long working distance, or by using smaller diameter SIL's so that a better short working distance lens could be used.

7 Engineering Diamond; Results and Discussion

7.1 Engineering Diamond 1

The engineering diamonds initially began with a number of test structures being milled by Mr R. Simmonds of the Optical Microscopy Group in Engineering, University of Oxford to produce damaged carbon regions.

The test structures were fabricated in ED1 and were a range of guides, wells and planes situated at different depths within the diamond, see Figure 6-7.

7.1.1 Pre-Anneal

7.1.1.1 Guide structures

Four guides were produced under different milling conditions.

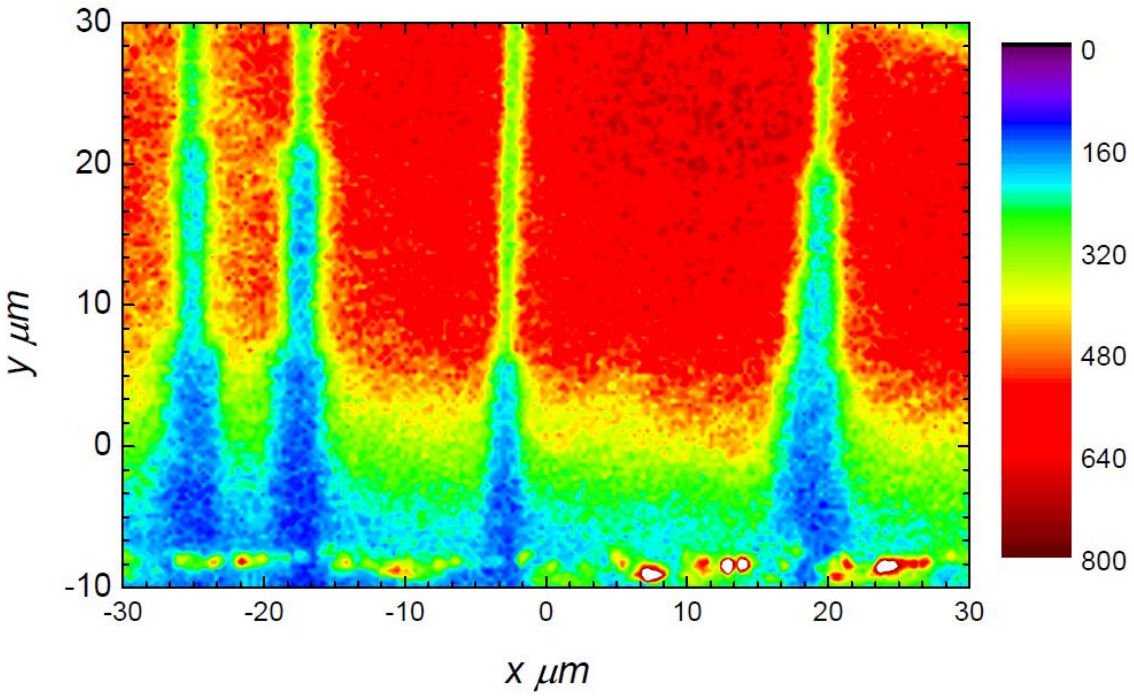

Figure 7-1 – False colour intensity map of ED1 guide ends imaged using the 100x lens on the scanning confocal microscope under 532nm excitation

Figure 7-1 shows the four guide ends as they reach the edge of the diamond. The guides have a low intensity of emission as the damaged diamond absorbs light; the majority of the

photoluminescence is produced by the raman emission of the bulk diamond (see Figure 7-6). Where the guides reach the edge of the diamond, the power of the milling laser must be increased to overcome the effects of reflection and refraction at the edge. As a result, the guides lose their definition and widen significantly. A line of brighter spots at the base of the contour map indicate the diamond edge, this is likely to be due to emission from contaminants.

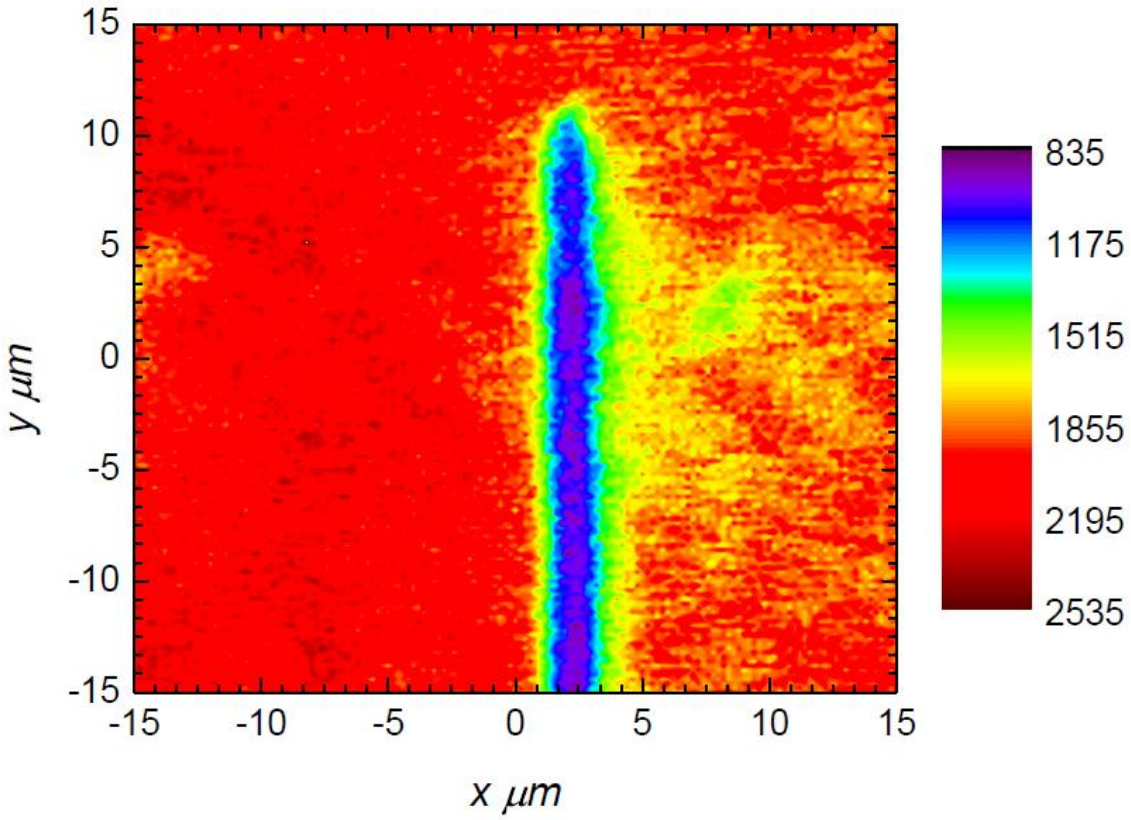

Figure 7-2 - False colour intensity map of ED1 guide ending in diamond bulk, imaged using the 100x lens on the scanning confocal microscope under 532nm excitation

Figure 7-2 shows the end of a guide ending in the bulk of the diamond, in comparison with Figure 7-1, the termination of the damaged diamond region is much cleaner. It is also clear from this plot that the guides are of a diameter of around 2-3 μm. This width was found to be consistent across all the guides.

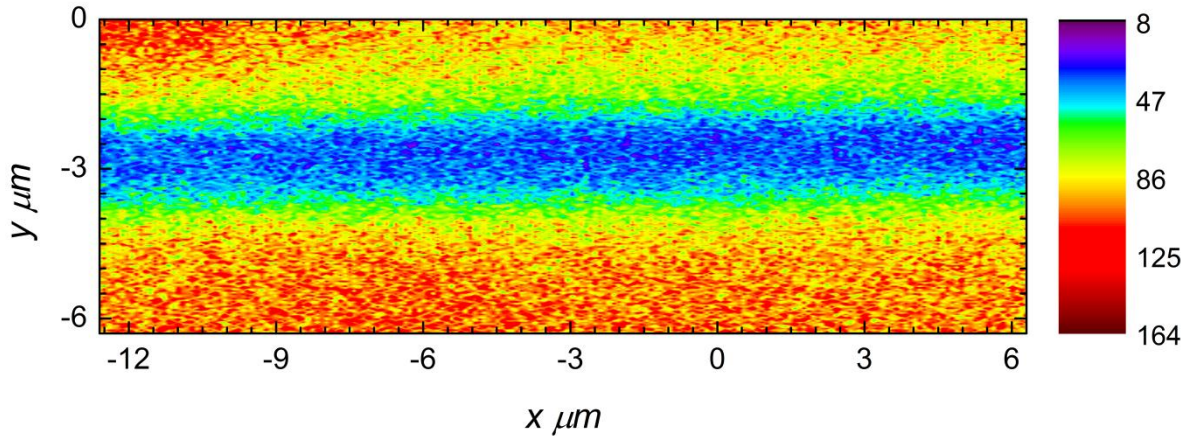

Figure 7-3 – False colour intensity map of ED1 guide in diamond bulk, imaged using the 100x lens on the scanning confocal microscope under 532nm excitation

Figure 7-3 shows a section of the central guide located in the bulk guide. Captured using low intensity laser excitation in order to reduce excitation of the bulk, this allows for the guide to be defined more sharply. The guide has a constant width along this 20 µm section; this is 1.6 µm and clarifies the information available in Figure 7-2.

7.1.1.2 Well Structures

A total of 10 wells were produced of varying milling parameters. Predominantly, the wells showed little change between one another in their diameter. As with the guides, the well's give little photoluminescence, this is again due to the lack of photon emission from the damaged diamonds. The resolution of images of the wells taken using the scanning confocal microscope is reduced by interference of the excitation by the walls of the wells. The wells are all imaged in the z plane, and fine focus is primarily achieved when observing the bottom face of the well

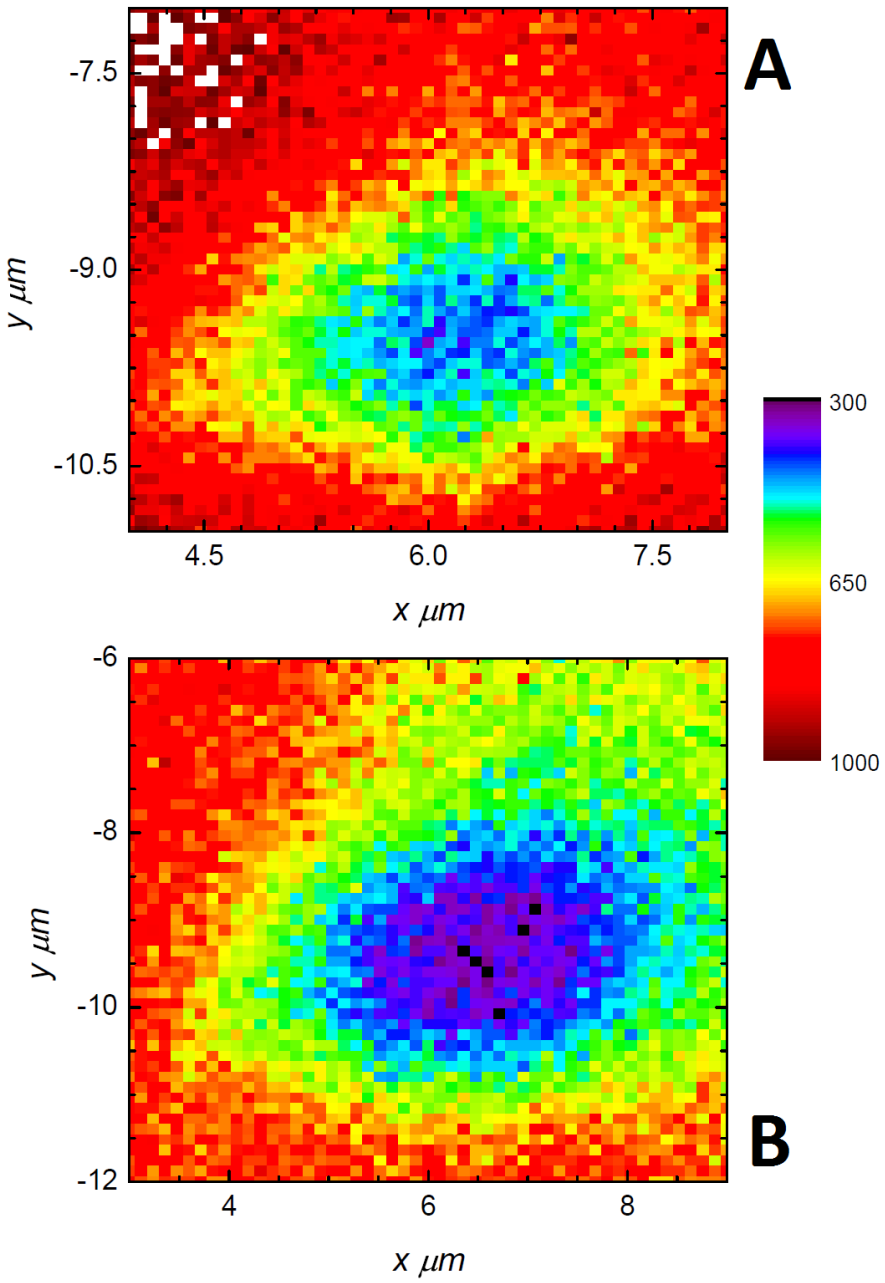

Figure 7-4 – False colour photoluminescence intensity maps of well structures in ED1; a well; imaged with the focal plane at the base of the well, 50 µm below the surface (A), and imaged with the focal plane halfway along the well, at a depth of 25 µm below the diamond surface (B), but otherwise under the same excitation conditions.

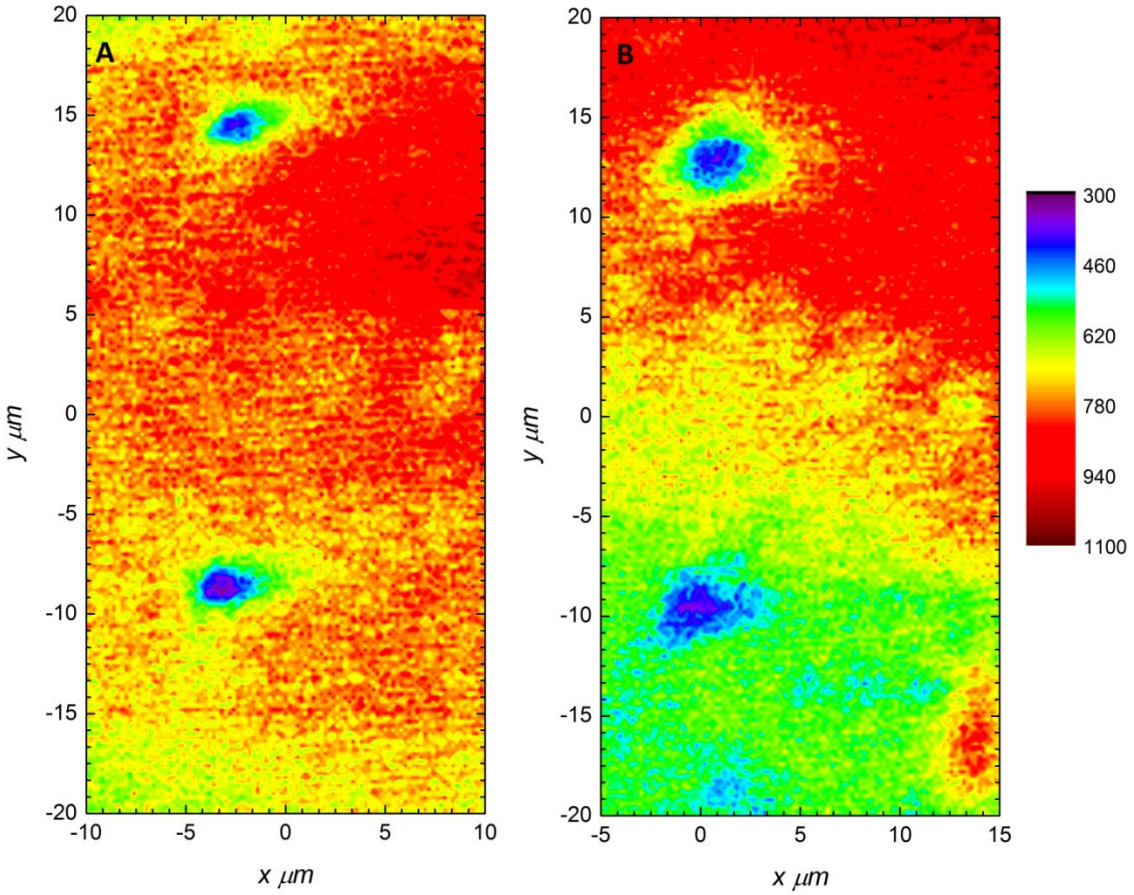

Figure 7-5 – False colour photoluminescence intensity maps of well structures in ED1; A shows wells closest to the plane structures; B shows wells closest to diamond edge. Both images are focused to a depth of 50 µm below the diamond surface.

The well structures shown in Figure 7-5 demonstrate typical results of the well milling. The wells are predominantly cylindrical, and are of diameter 3 µm, the wells show fairly constant diameter with depth, tapering to a blunt tip in the deepest 5 µm.

The wells show uniform dimensions given different milling rates as seen in Figure 7-5, the anomalous result in B being the lower image where the milling parameters were incorrect and the well was milled with an elliptical cross section.

Spectral information obtained from ED1 shows a high concentration of NV centres in the sample (see Figure 7-6). Spectra were obtained between features, at features and at a distance of more than 2 mm away from any milled features, under identical excitation conditions. It was observed that the

intensity of NV centre emission was increased in the vicinity of the milled features, this suggests that the milling process leads to the creation of more NV centres in the diamond. This may be due to the strain introduced by the formation of the amorphous carbon during milling. It may be expected that the milling process is a heating process, however, Mann, et al. reported that the mechanism of material damage is a multiphoton process [71] and this is now accepted as the most likely method [51] [54]. A likely reason for this effect is thus that the amorphous carbon takes a larger volume than the diamond it replaces, so a compressive strain is applied in the diamond. This provides a driving force for the diffusion of vacancies toward the milled features, leading to the creation of NV centres where the local strain field interacts with the local strain field of the substitutional nitrogen atoms.

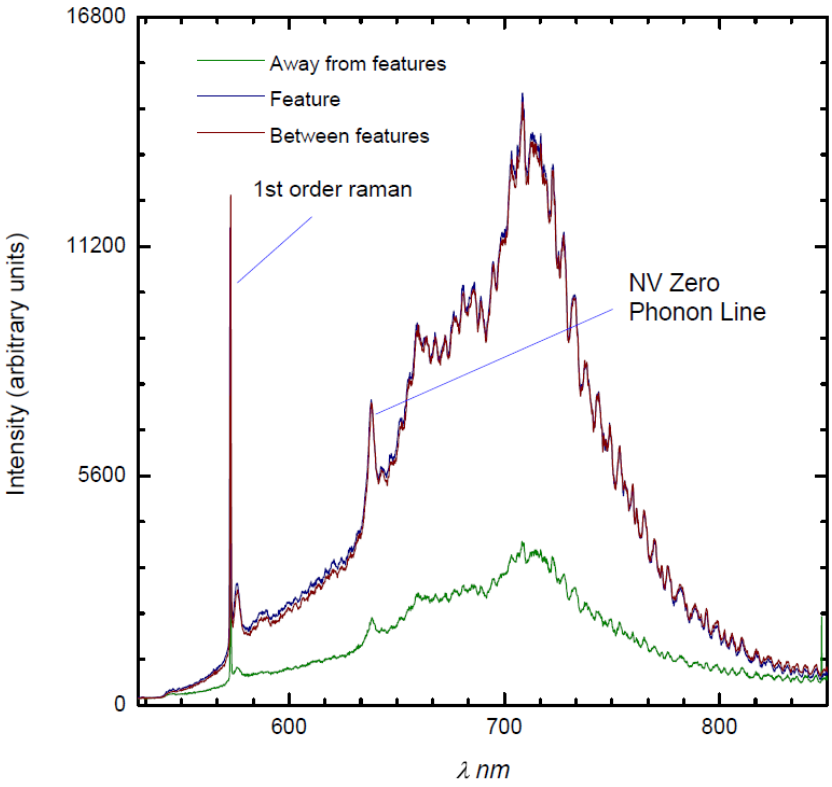

Figure 7-6 – Spectra from ED1, all 60s exposures under the same excitation conditions. Strong Raman signal is observed from the diamond bulk at 567 nm and NV centres are present given by the presence of the NV zero phonon line (ZPL) at 637 nm.

7.1.1.3 Planar Structures

Two planar structures were milled, one at a depth of 5 µm and one at a depth of 50 µm. The two structures measured approximately 25 µm by 15 µm.

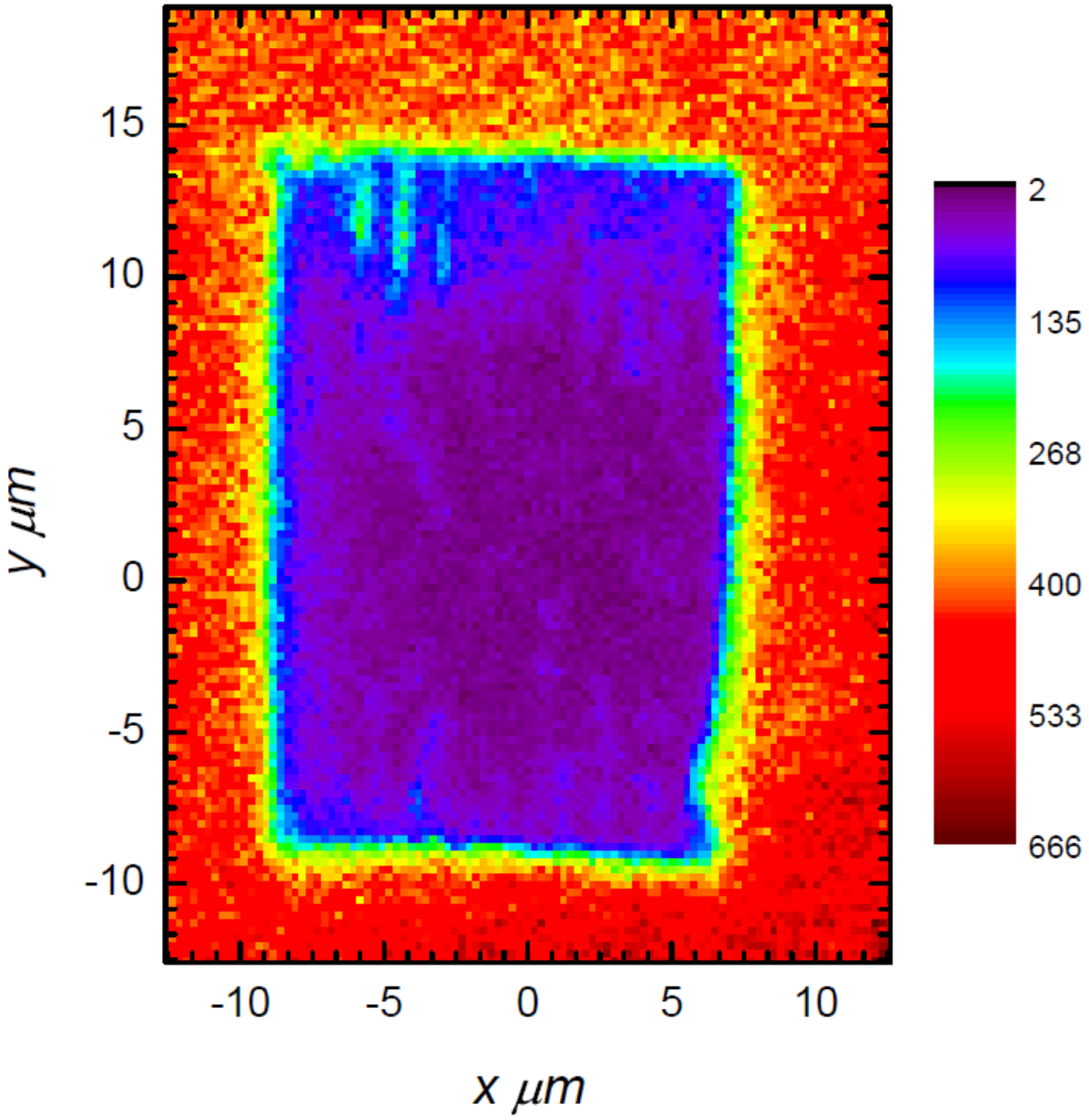

Figure 7-7 – False colour photoluminescence intensity map of plane structure in ED1 milled at a depth of 5 µm below the diamond surface.

Figure 7-7 shows the shallow plane milled at a depth of 5 µm, there are vertical wells extending from each corner to the surface. The structure is reasonable uniformly milled, however it is apparent

that in a small section (around coordinates (-5, 10)), the milling has not completely joined up, the plane is thus incomplete and it is possible to see the passes made by the focused laser.

In contrast, the deeper well in Figure 7-8 shows much better continuity of the plane. This suggests that some work is required to perfect the aberration correction of the milling device at shallower depths of milling.

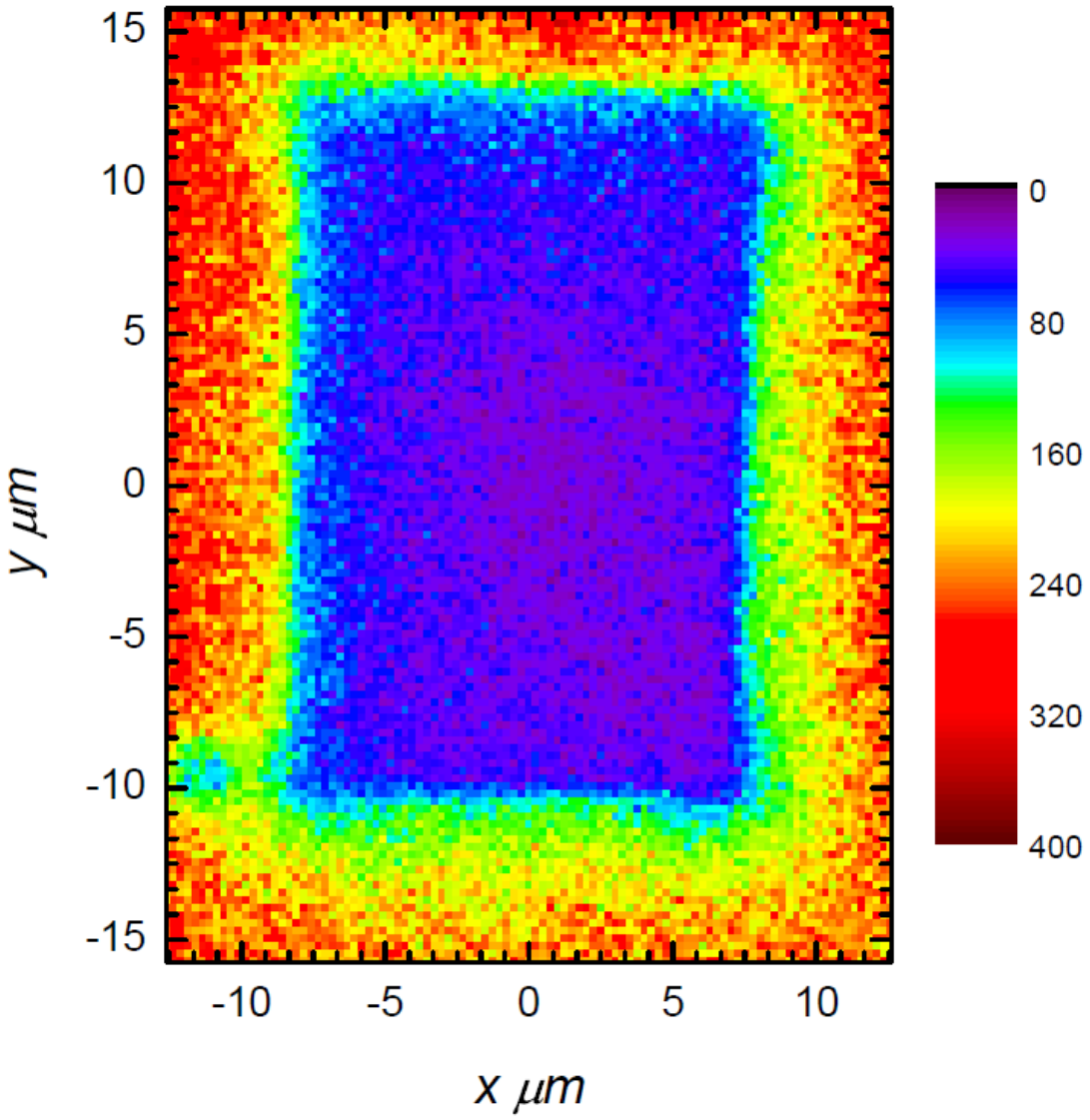

Figure 7-8 – False colour photoluminescence intensity map of plane structure in ED1 milled at a depth of 50 µm below the diamond surface.

7.1.2 Post Anneal

Following annealing the diamond had a smoky-grey discolouration (see Figure 7-10). This is attributed to some of the carbon at the surface decomposing to graphite and on closer inspection it is possible to see additional deposition of material. The distribution of deposits is even across the diamond surface and appears as a film of material with larger deposits from place to place. On viewing the diamond with the SCM; it is not possible to examine any subsurface features owing to the surface contaminants introduced during annealing (see Figure 7-9).

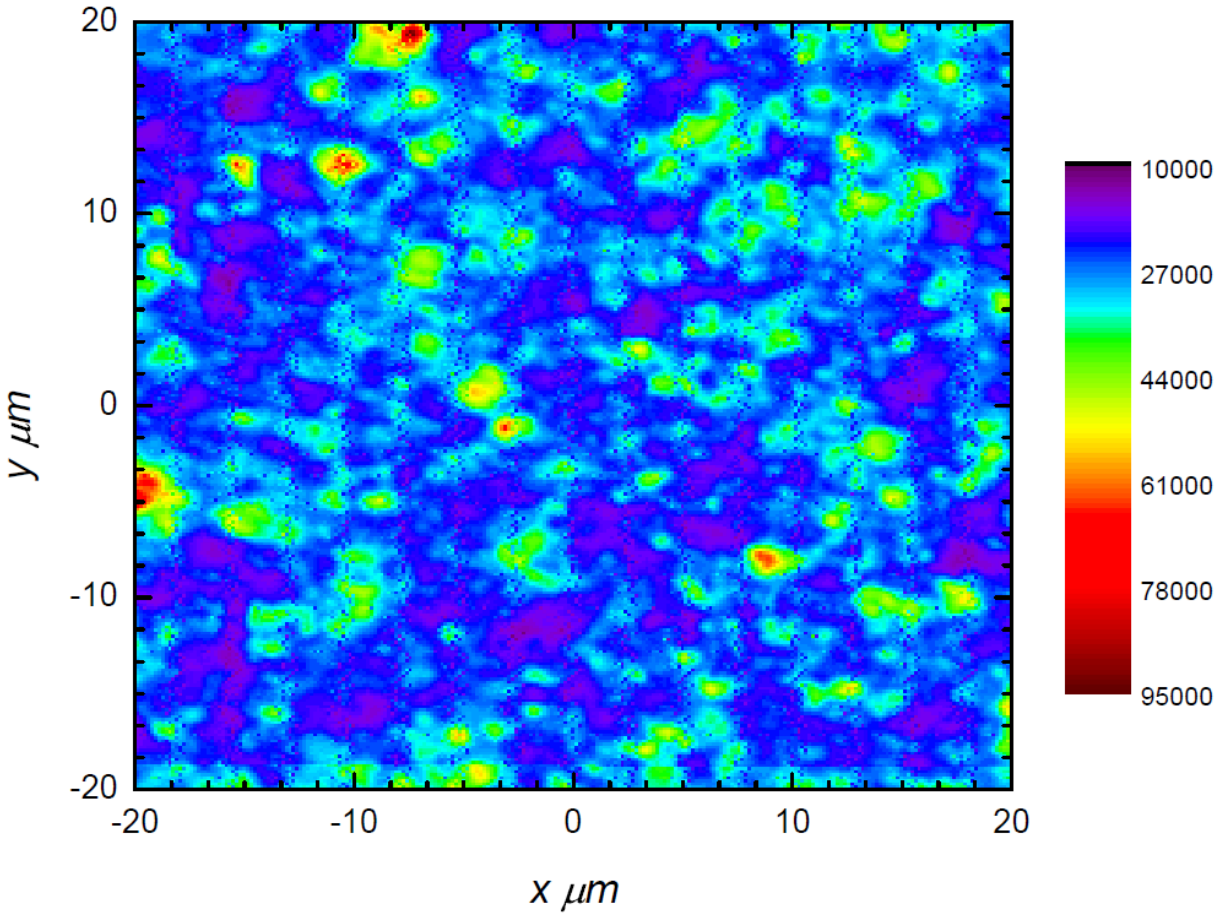

Figure 7-9 – False colour photoluminescence intensity map of two wells imaged at a depth of 50 µm after annealing and an aqua regia soak and boil. It is impossible to distinguish the feature owing to the photoluminescence of surface contaminants. Note also the presence of artefacts from the SCM software in the way of regular arrays of dark pixels followed by light pixels.

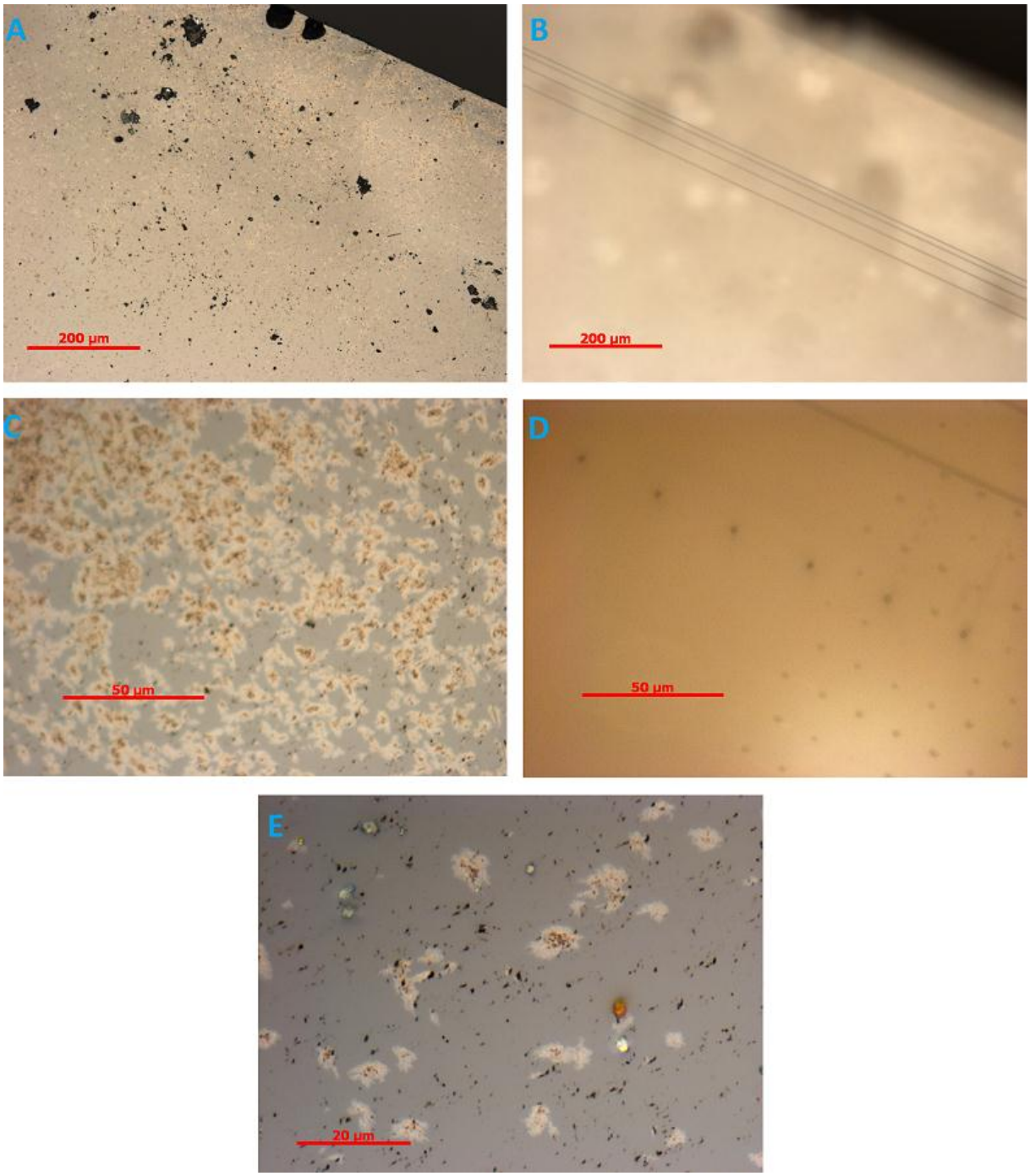

Figure 7-10 – Optical micrographs in reflection mode of the surface and features of ED1 post-anneal and aqua regia boil. A is the diamond surface, B shows the underlying guide structures at the same position. C is the diamond surface, and B the underlying well structures at the same position. E shows the surface structures over the guides at the same position as A and B, it was not possible to resolve the guides.

7.2 Engineering Diamond 2

7.2.1 Pre-Anneal

Following what was learnt from the fabrication of structures in ED1, a number of new structures were designed and built for a second diamond of similar properties to the first, ED2 had a similar concentration of NV centres to ED1 and was of the same dimensions. Spectra were recorded across the sample and were all of the form shown in Figure 7-11, showing strong raman emission, and strong NV centre emission, indicated by the sharp peak at 637 nm (the zero phonon line).

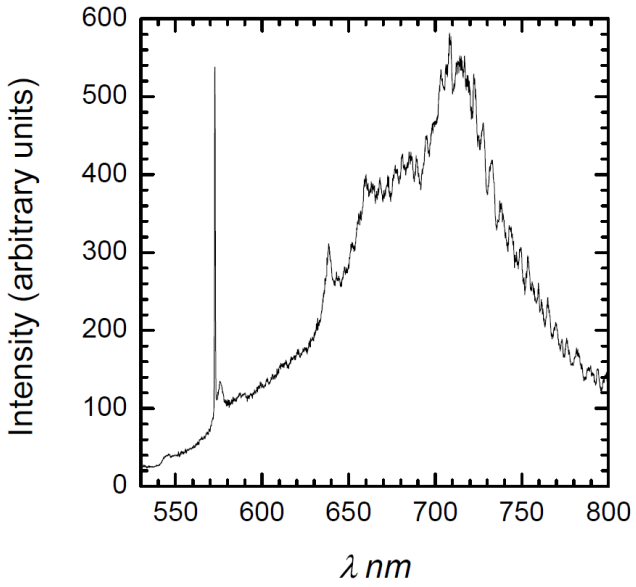

Figure 7-11 – Spectrum taken in bulk of ED2, 30s exposure.

The sample was milled under the same conditions as ED1, with new structures as shown in Figure 6-8. A number of different structures were attempted including; rib waveguides in an attempt to replicate the work of Hiscocks, et al. [40] using the dual aberration corrected laser milling [54]; electrical guides to allow tuning of the ground state of the NV centre; and, a plate capacitor device. All the structures were designed with electrochemical etching in mind to remove the graphite (see sections 7.3 and 4.4.4).

The structures were imaged using optical microscopy prior to annealing.

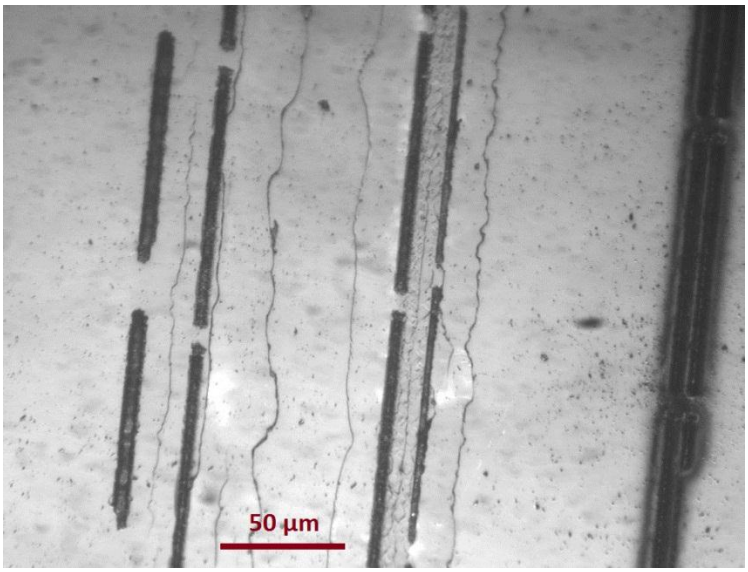

Figure 7-12 – Optical micrographs of ED2, taken prior to annealing, of three rib guides milled; from left to right, structures 1, 2, and, 3 (all from Figure 6-8). Taken in reflection by Mr R. Simmonds.

Figure 7-12 shows milled waveguides, with a large amount of structural damage within the diamond. This is due to the expansion of the amorphous carbon on formation, as proposed in section 7.1.1.2. This effect is prevalent in only the two larger rib waveguides, where the amount of amorphous carbon has a large volume; the smaller waveguides are largely unaffected due to smaller strain fields.

Figure 7-13 shows an improvement over the guides of ED1, the control of milling is much better, and sharper structures have been milled. The guides milled are below 2 µm in width and are well resolved. This should give good optical properties as the sidewalls are smoother, leading to less absorption losses. The three structures of A, B and C demonstrate the high level of control possible with the dual aberration corrected laser milling, with tolerances of sub-micron order.

The electrodes displayed in Figure 7-14 are designed to allow for good electrical connections to be made mechanically to the diamond surface so that electrolysis of a solution could be utilised to remove the graphite by oxidation. The size of the electrodes is around 20 µm by 50 µm, these are present on all structures milled. It was observed in some areas that the weak bonding of the

amorphous carbon layers caused them to be removed during simple cleaning processes such as acetone washes; so leaving a pit with amorphous carbon at the base.

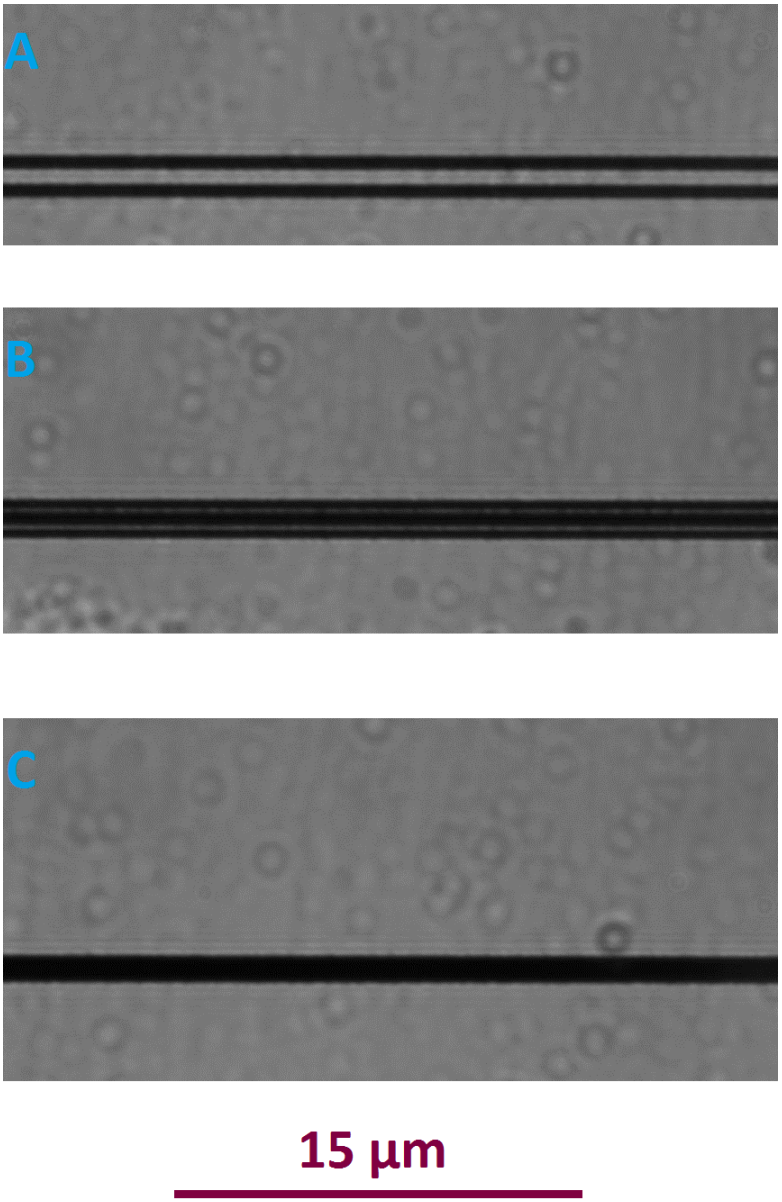

Figure 7-13 - Optical micrographs of ED2, taken prior to annealing, of three tracks milled; A is structure 6, B is structure 7, C is structure 8 (all from Figure 6-8). All taken using an oil immersion lens with NA=1.4 by Mr R. Simmonds.

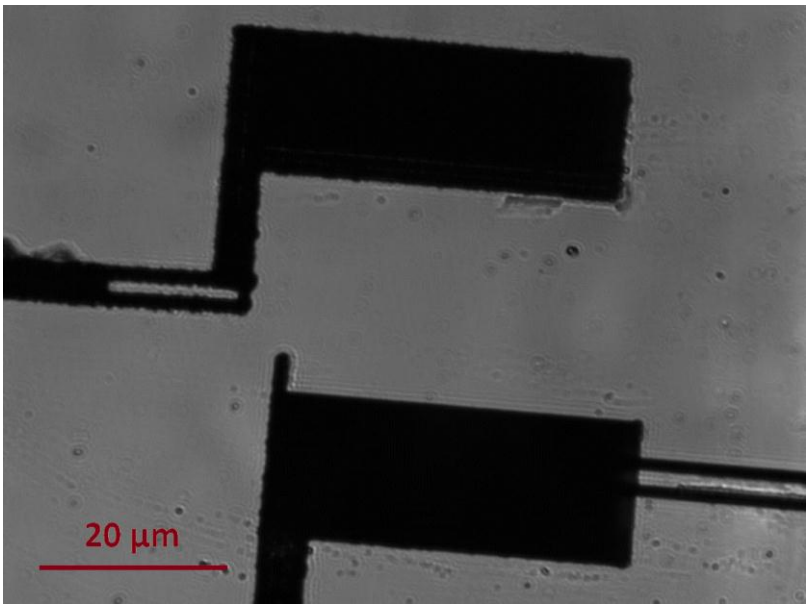

Figure 7-14 – Optical micrograph of electrode structures on ED2, designed to allow easy electrical connection of structures for graphite removal, electrodes of structures 3 and 4 (referring to Figure 6-8). Taken in transmission by Mr. R. Simmonds.

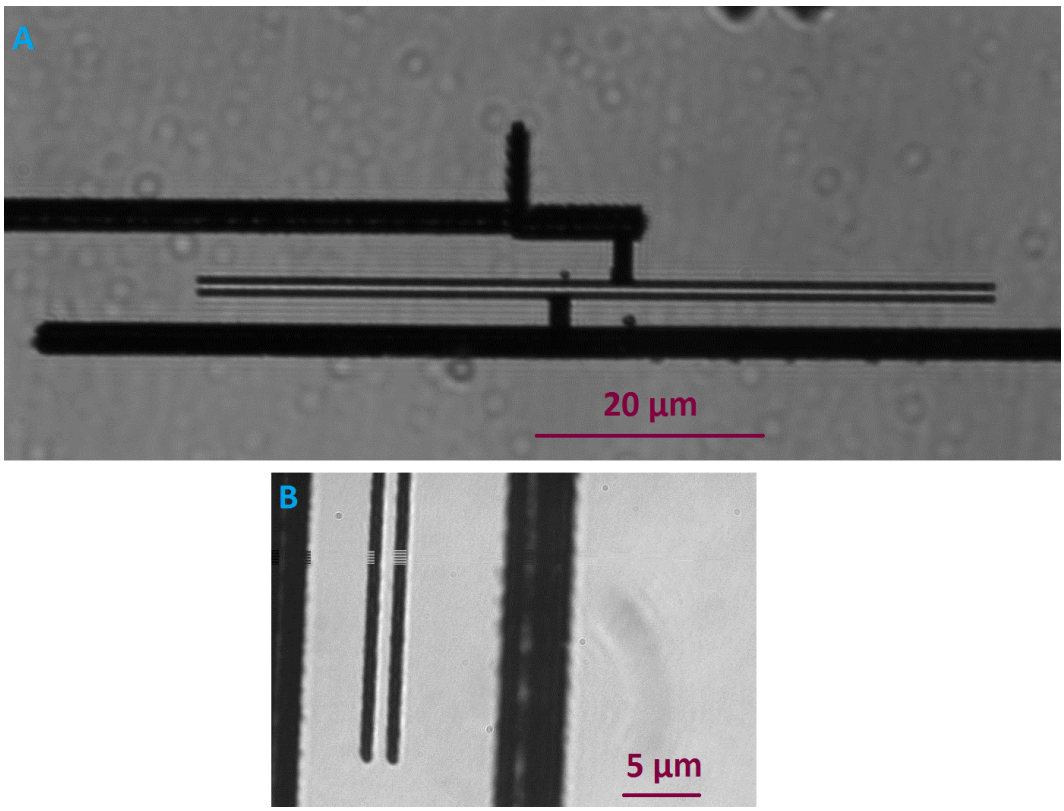

Figure 7-15 – Optical micrographs of ED2 taken prior to annealing of the capacitor device (structure 12 in Figure 6-8) separation of the plates is 1 µm. A was obtained with an lens with NA=0.9, B obtained using an oil immersion lens with NA=1.4. Both taken Mr R. Simmonds.

The capacitor device of Figure 7-15 is a construction to high tolerances; the depth of the plates is 160 µm and the width 70 µm, with a distance between the plates of 1 µm. Assuming the parallel plate model for capacitance, where the capacitance, *C,* is proportional to the area, A, of the plates and the separation between the plates, *d*,

$$C = \frac{\varepsilon A}{d}$$

Given a relative permittivity, ε_r, of roughly 10 for diamond, we can expect a capacitance of the order of 1 nF for the device constructed. It was not possible to obtain an experimental value owing to shorting of the guides by the graphite surface film that arose from annealing.

7.2.2 Post anneal

ED2 was annealed at 1100°C in vacuum for 1 hour. As with ED1, the diamond has a noticeable grey discolouration after annealing; by direct comparison ED2 was darker in tone. The diamond was soaked for 48 hours in aqua regia, then boiled for two hours in fresh solution, no noticeable change was observed.

Optical micrographs were taken of the surface and features. It was observed that there were a much larger number of fractures in the diamond in the areas noted above (see Figure 7-12) and these fractures extended into the surface guide structures 1 through 5 (see Figure 7-17 and Figure 7-18). It was also observed that in some places that flakes of diamond had fallen off completely. In addition to this damage, there were more surface defects noted in the direct vicinity of the fractures, especially deposition of large areas of material (see Figure 7-16).

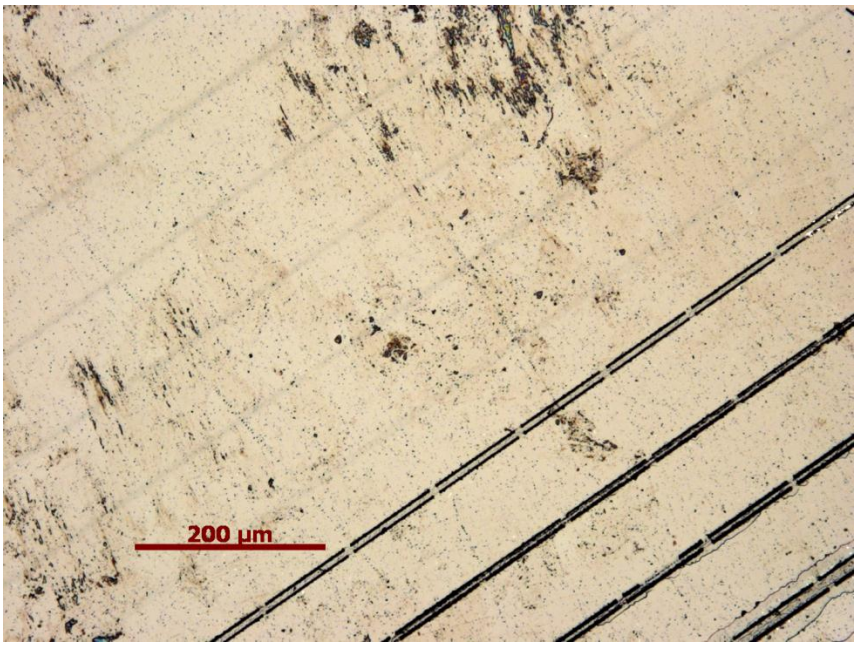

Figure 7-16 – Reflection optical micrograph of guides and tracks 11 to 2 (working rightwards from top left-hand corner). Fractures are visible in guides 2, 3 and around 4. A large amount of surface deposition is also visible.

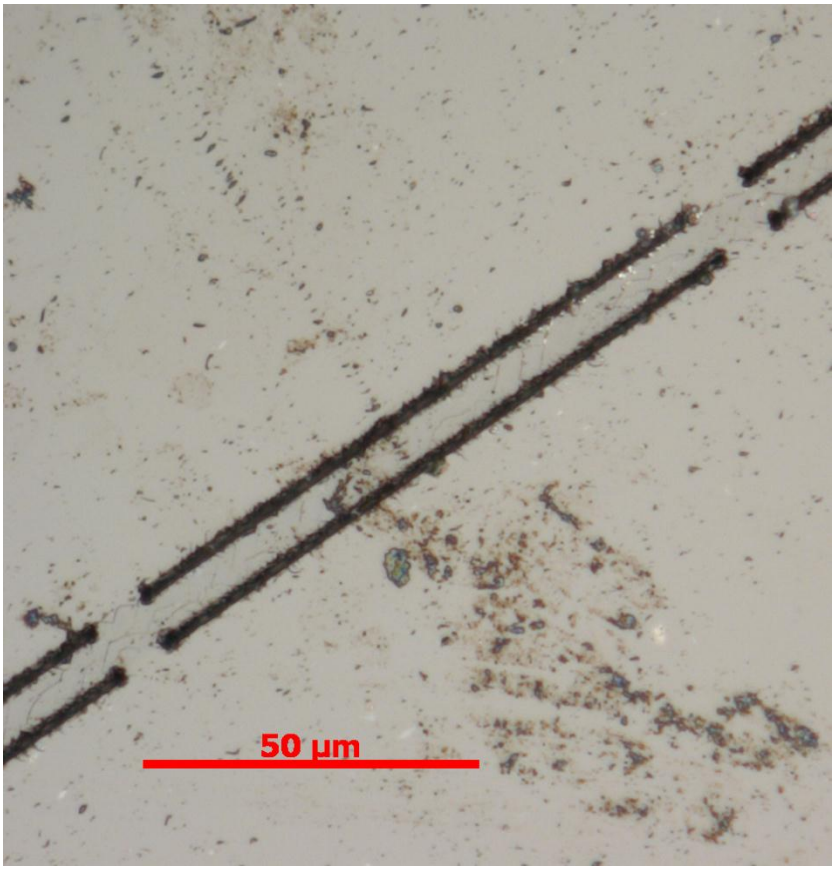

Figure 7-17 – Reflection optical micrograph of guide 5. Fractures in the bulk diamond are readily visible in the centre of the rib, and extending away from the milled sections along the diamond surface.

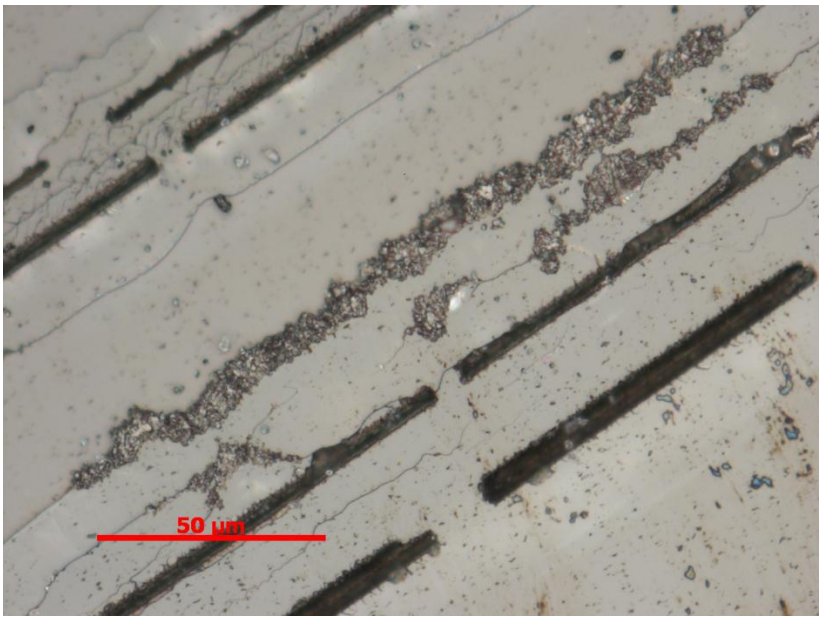

Figure 7-18 – Reflection optical micrograph of guides 1 and 2. A high density of surface fractures are visible between the guides and alongside them. A large amount of material has been deposited over the fractures during annealing.

7.3 Electrochemical etching

In order to remove the graphite from ED1 and ED2, a number of methods were investigated, the most prominent being the possibility of electrochemically etching the graphite, making use of its conductivity, whilst the diamond has a very high resistance so would be unaffected.

Tests were performed on a graphite rod to simulate the conditions the graphite in diamond would be put under and to obtain a reasonable measure of the feasibility of electrochemical etch. Three solutions were used, hydrochloric acid, boric acid (as suggested in the literature [40]) and sodium hydroxide to examine the effect of pH on the reactions.

In reference to Figure 7-19, the hydrochloric acid polarisation curve showed a notable active peak at around 400 mV of potential. This was apparent in the forward and reverse polarisation in both the anodic and cathodic reactions and offers a region for successful removal of carbon. It was investigated to ensure that it was not an effect of capacitance in the rod from the surface layer, and results indicate that it was not. Boric acid has a small active region, but the current did not reach that

achieved by the hydrochloric acid whilst in the active region. The sodium hydroxide showed a similar active region to the boric acid, albeit at a slightly lower current and at a negative potential.

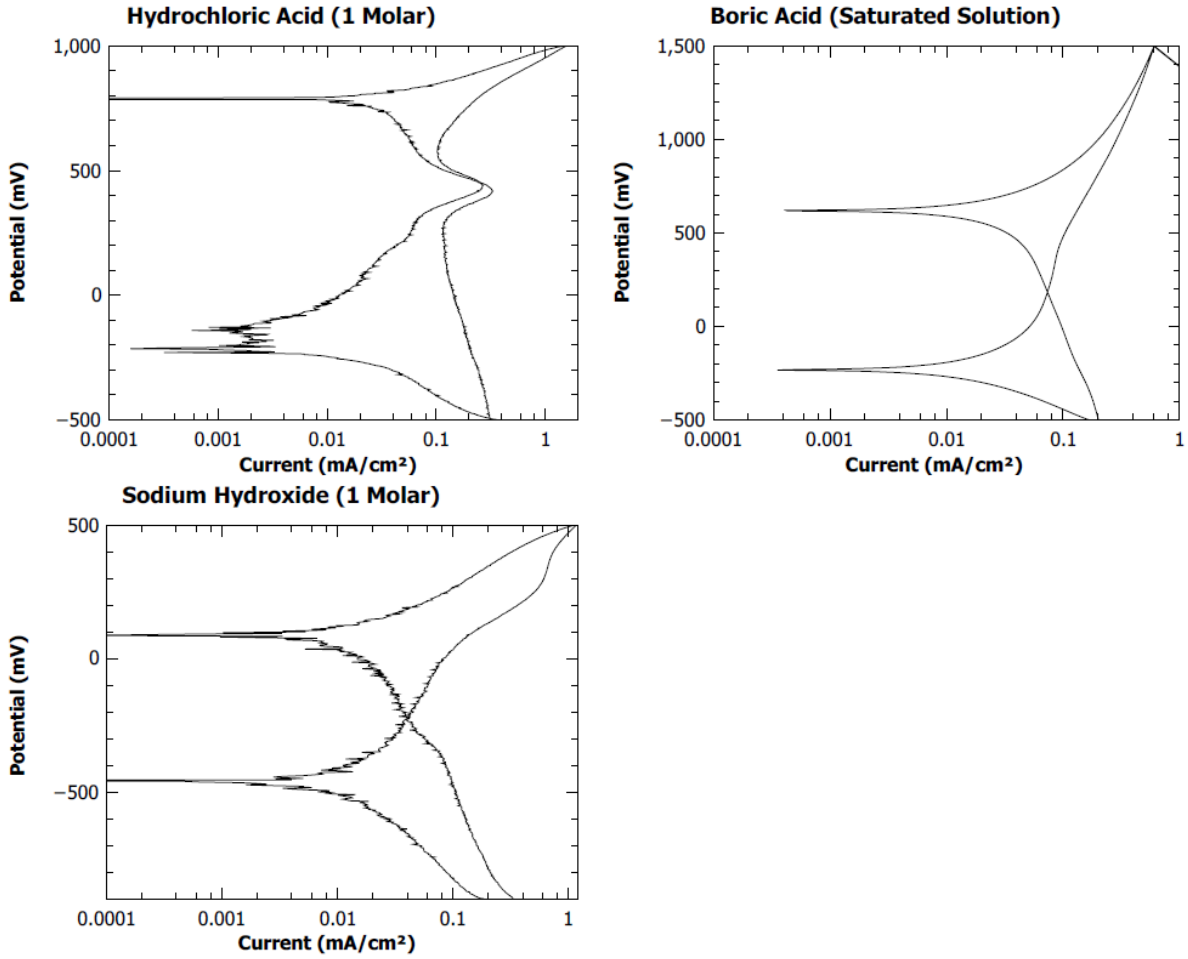

Figure 7-19 – Polarisation curves for a graphite rod in various solutions as a simulation of the performance of graphite. The curves were taken at room temperature at a sweep rate of 200mV/min, with a graphite electrode, steel electrode and a calomel reference electrode

8 Nitrogen Vacancies in Diamond; Results and Discussions

8.1 Solid Immersion Lenses

The solid immersion lenses were examined in order to evaluate their ease of use and the effects they have. PCTF was the primary sample examined.

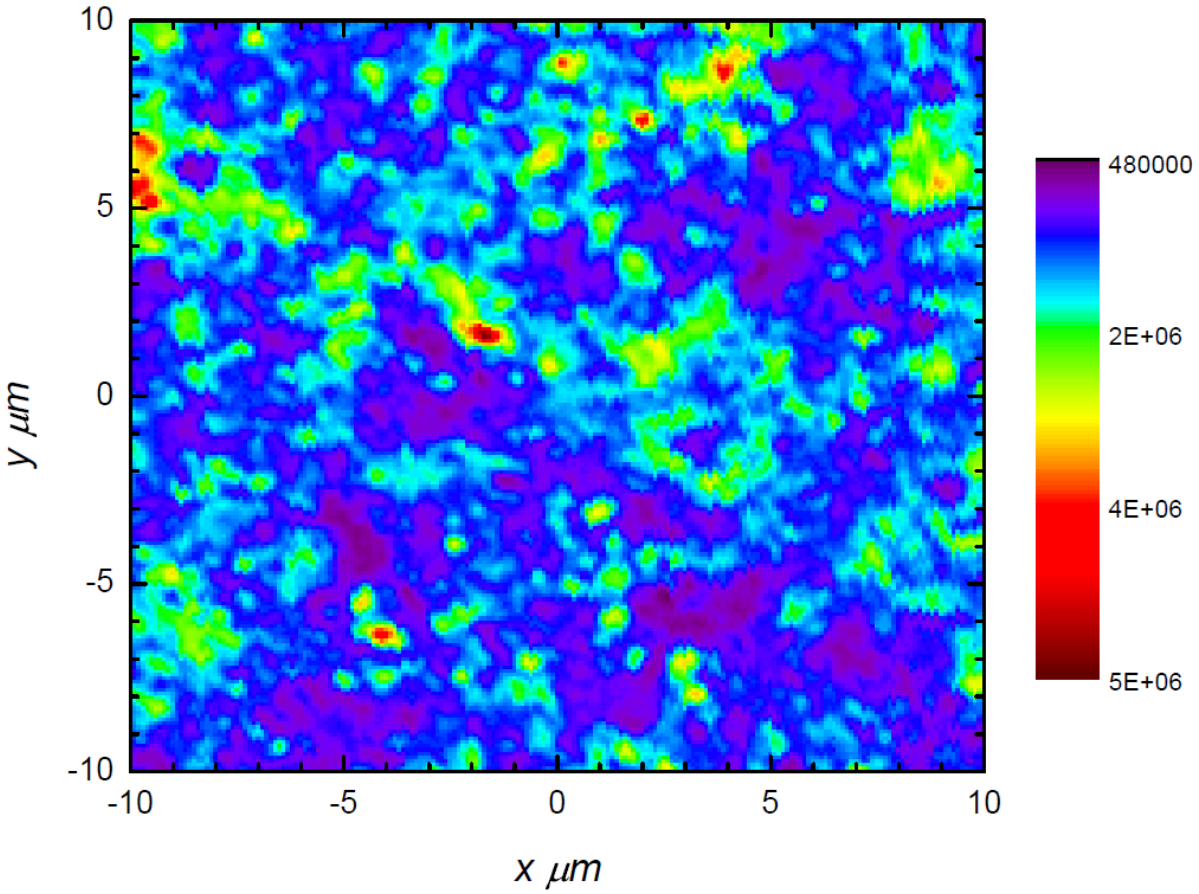

Figure 8-1 – False colour photoluminescence intensity map of PCTF, characteristic of all areas examined in sample. The bright features are stable; there is shift in the *y* direction in the image due to noise from vibration of the optics bench. Taken using 100x lens through air.

In Figure 8-1 there are a large number of defect centres present in PCTF, these are found to be continuous across all depths of the film. The defect centres were found to be stable under high power laser excitation and showed no bleaching. In addition, the brightest regions were able to emit in excess of 100×10^6 photons per second if sufficiently excited, it would be expected that a single NV centre at saturation could emit of the order of 10^4 photons per second [48]; showing that there is a

very high concentration of emitters in this sample. Figure 8-2 is typical of spectra obtained from this sample, showing strong NV emission with the ZPL at 637 nm and a distinguished phonon side band.

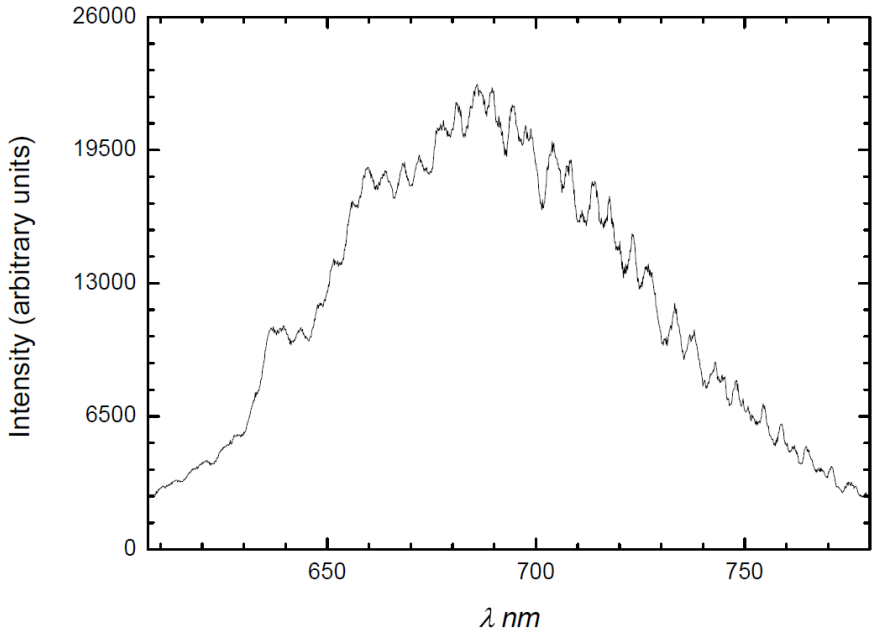

Figure 8-2 – Characteristic spectrum from point (-2,2) in Figure 8-1, 60s exposure. No raman signal was recorded owing to the thickness of film. Near identical spectra were recorded throughout the PCTF.

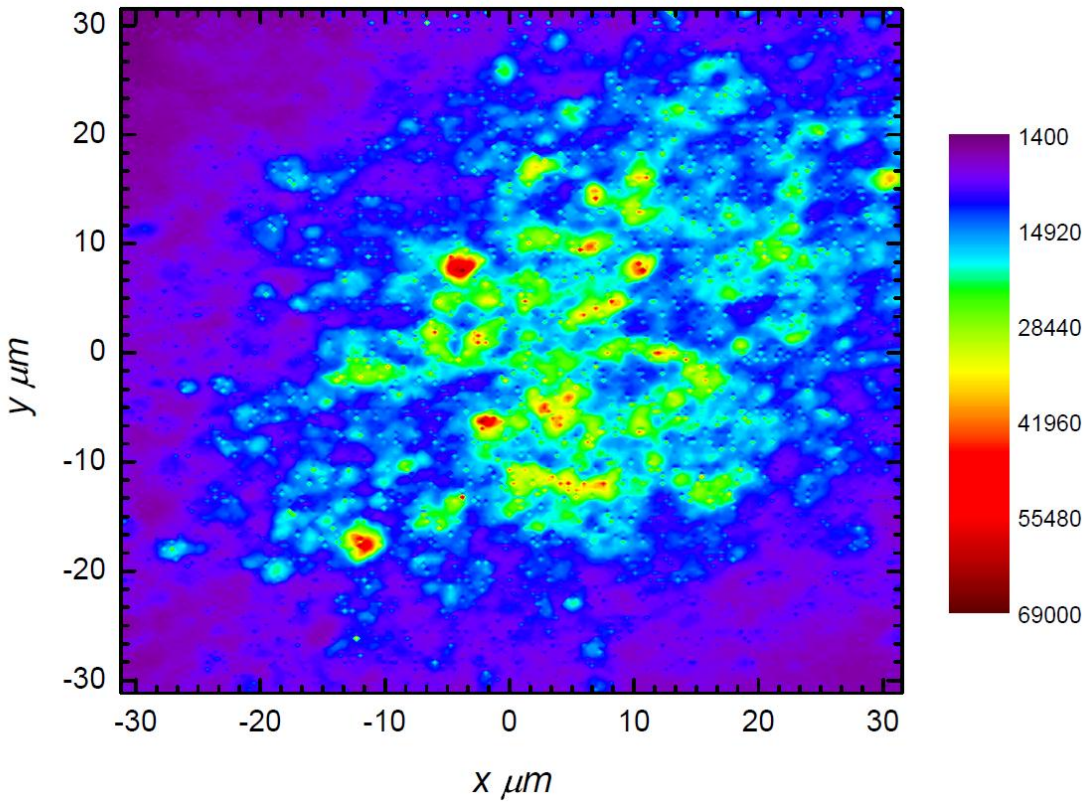

Figure 8-3 – False colour photoluminescence intensity map of PCTF with sSIL on surface. Taken using the 50x, long working distance lens. Note the presence of array artefacts from recording software.

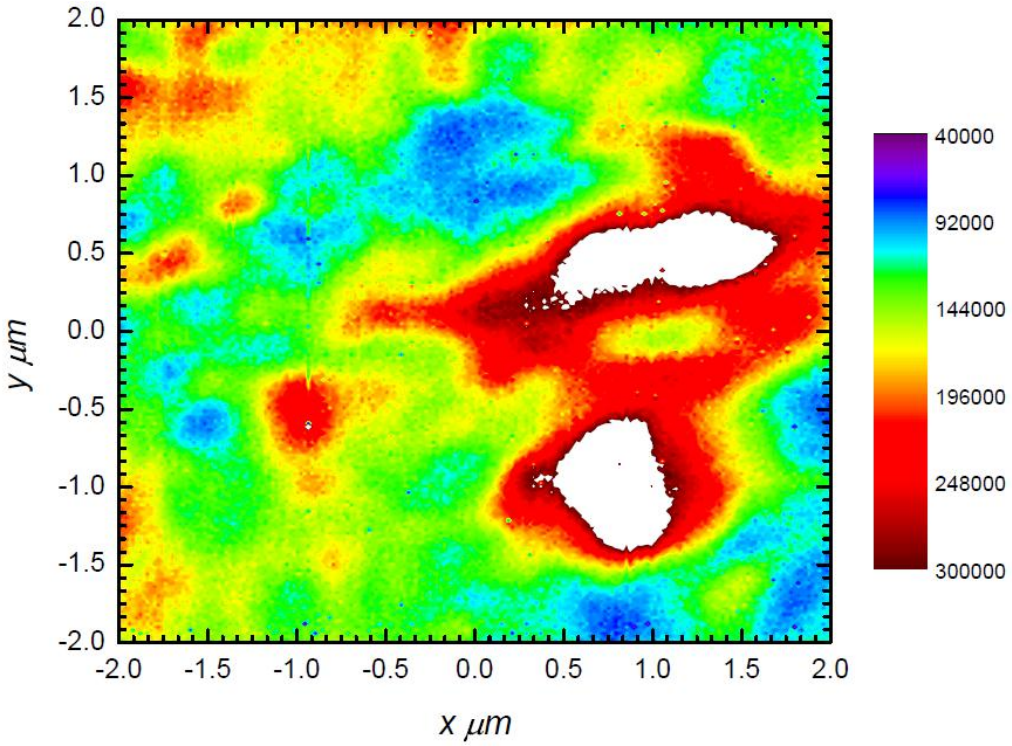

Figure 8-4 – False colour photoluminescence map of small features in the PCTF using the sSIL. Taken using the 50x long working distance lens. The colour scale has been adjusted to highlight particular featurs.

The addition of the sSIL to the PCTF demonstrates a number of key points. In Figure 8-3 the central region that is closest to the second aplanatic focal point (see section 4.3.1.1) shows enhancement of emission over the areas around it. However, owing to the difficulties in obtaining good, flat contact between the sSIL and PCTF and the refraction losses at the interface it has not been possible to obtain the increase in NA of n^2 as reported in the literature [32] [33] [30]. It has been possible to demonstrate the improvement in resolution due to the increase in the effective NA of the system. In Figure 8-4 a bright spot at (-1.3, 0.7) has a size of 150 nm at its narrowest. This approaches the theoretical limit of 133 nm.

It was not possible to find any isolated NV centres in the PCTF. The closest obtained and imaged with the sSIL in place is shown in Figure 8-5, its NV emission is verified by the distinct ZPL at 637 nm in Figure 8-6. On taking a Hanbury Brown and Twiss measurement, it was found that there were more than 5 individual centres emitting when the excitation was placed over the (0, 0) bright spot.

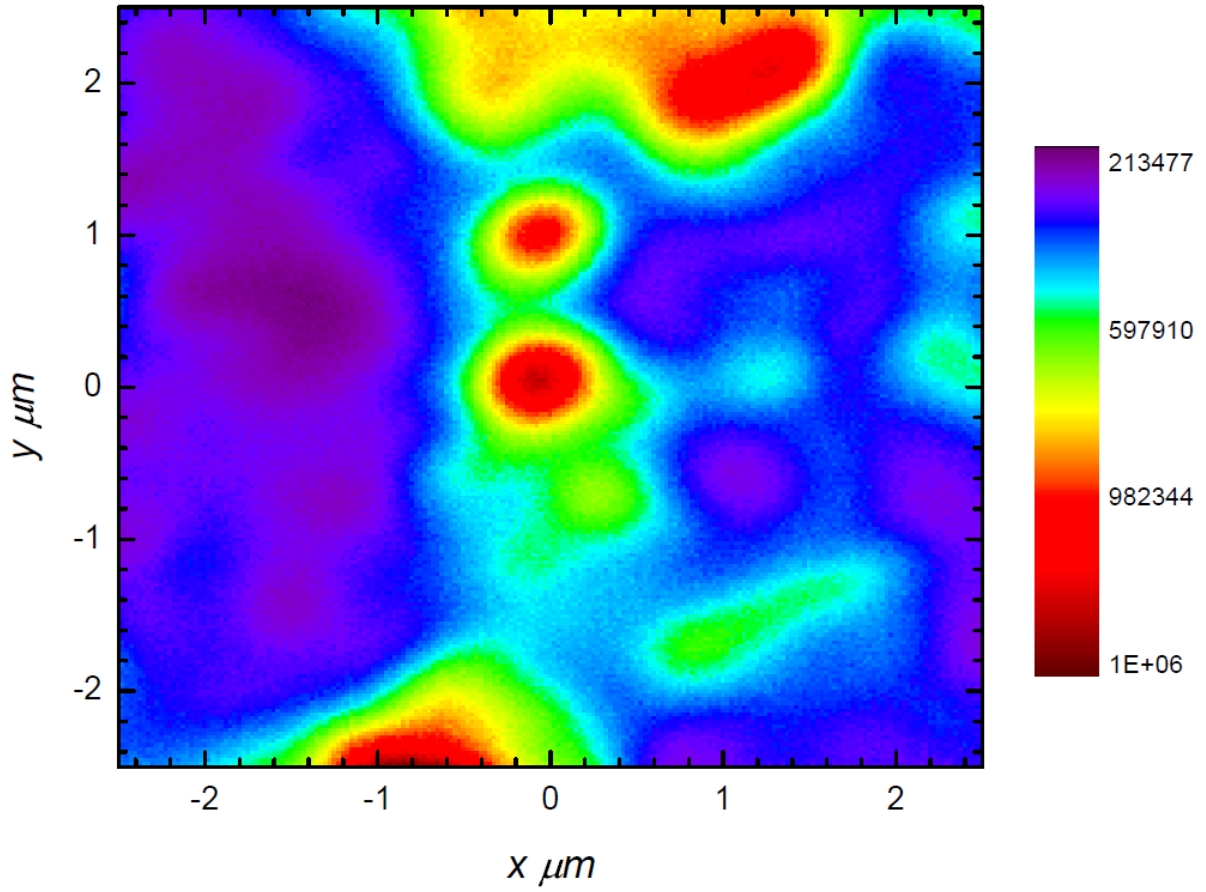

Figure 8-5 – False colour photoluminescence map of bright features in PCTF, viewed with sSIL.

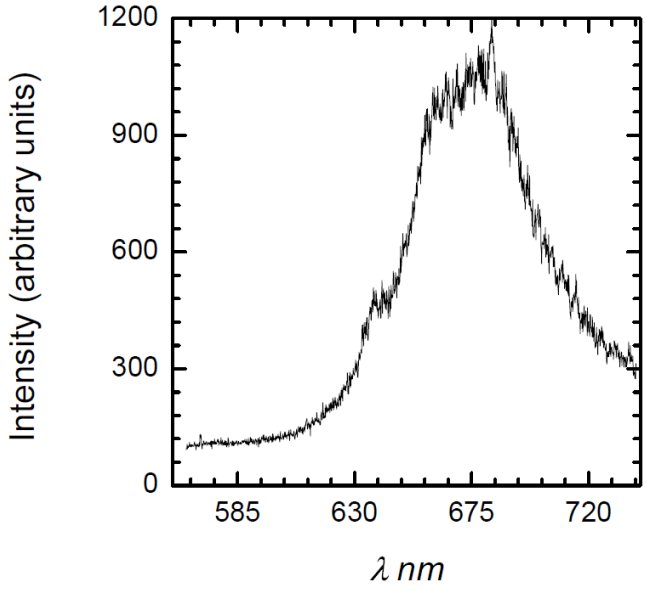

Figure 8-6 – Spectrum of the bright spot centred at (0,0) in Figure 8-5.

8.2 Polycrystalline Diamond Slab

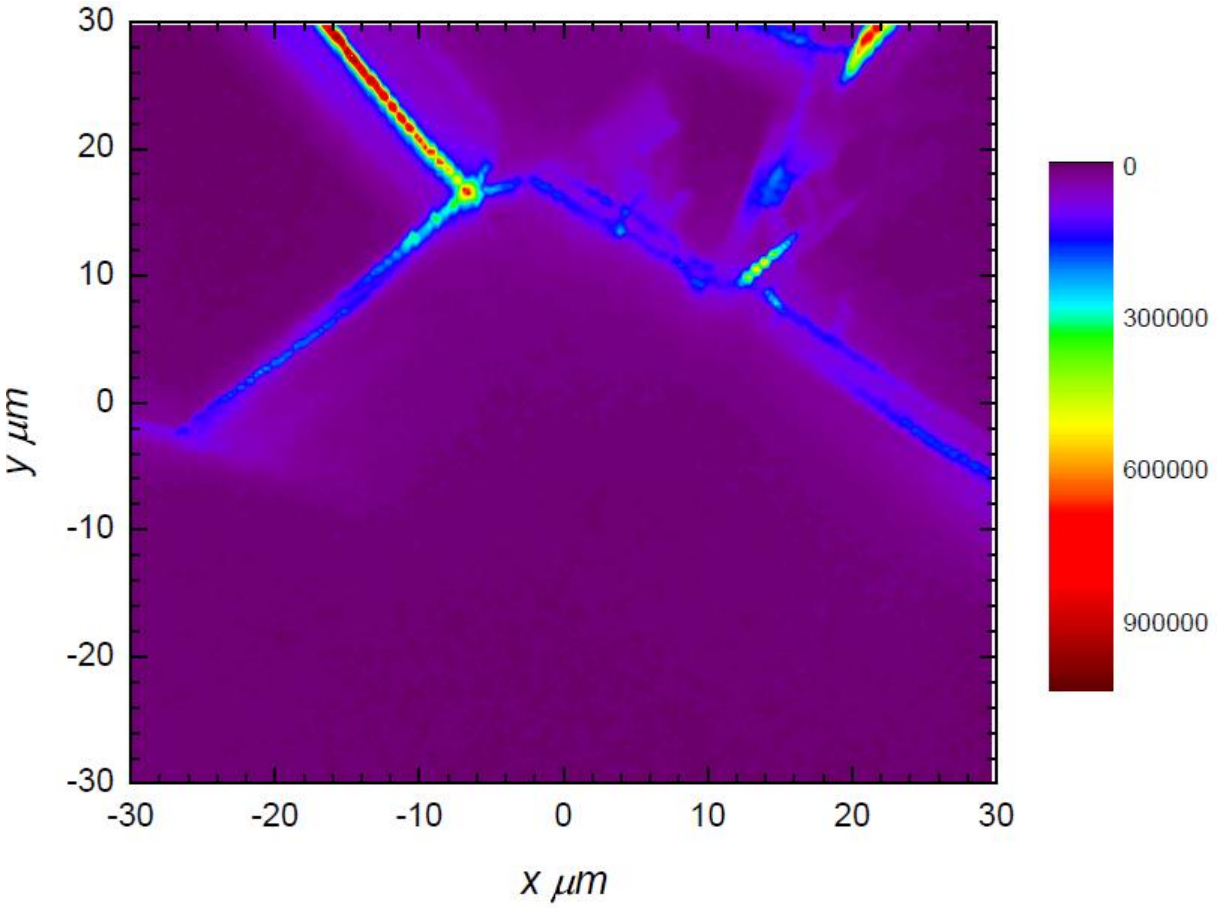

Figure 8-7 – False colour photoluminescence map of typical structures observed in PCDS. Obtained using 100x lens. The bright areas are grain boundaries with a high concentration of NV centres.

Figure 8-7 shows the typical photoluminescence observed in the polycrystalline diamond slab. The grain boundaries contain a very high concentration of NV centres; individual centres are not resolved in these areas. The centres of the grains have very low NV concentration, it is expected that there should be isolated single defect centres in these regions, but none have been identified. Comparisons with Figure 8-1 show a stark contrast in the distribution of NV centres despite both being polycrystalline samples. This may be a result of the differences in the synthesis of the two diamonds, though no specific information is available as to the exact conditions of synthesis for either sample.

8.3 Implanted Diamond

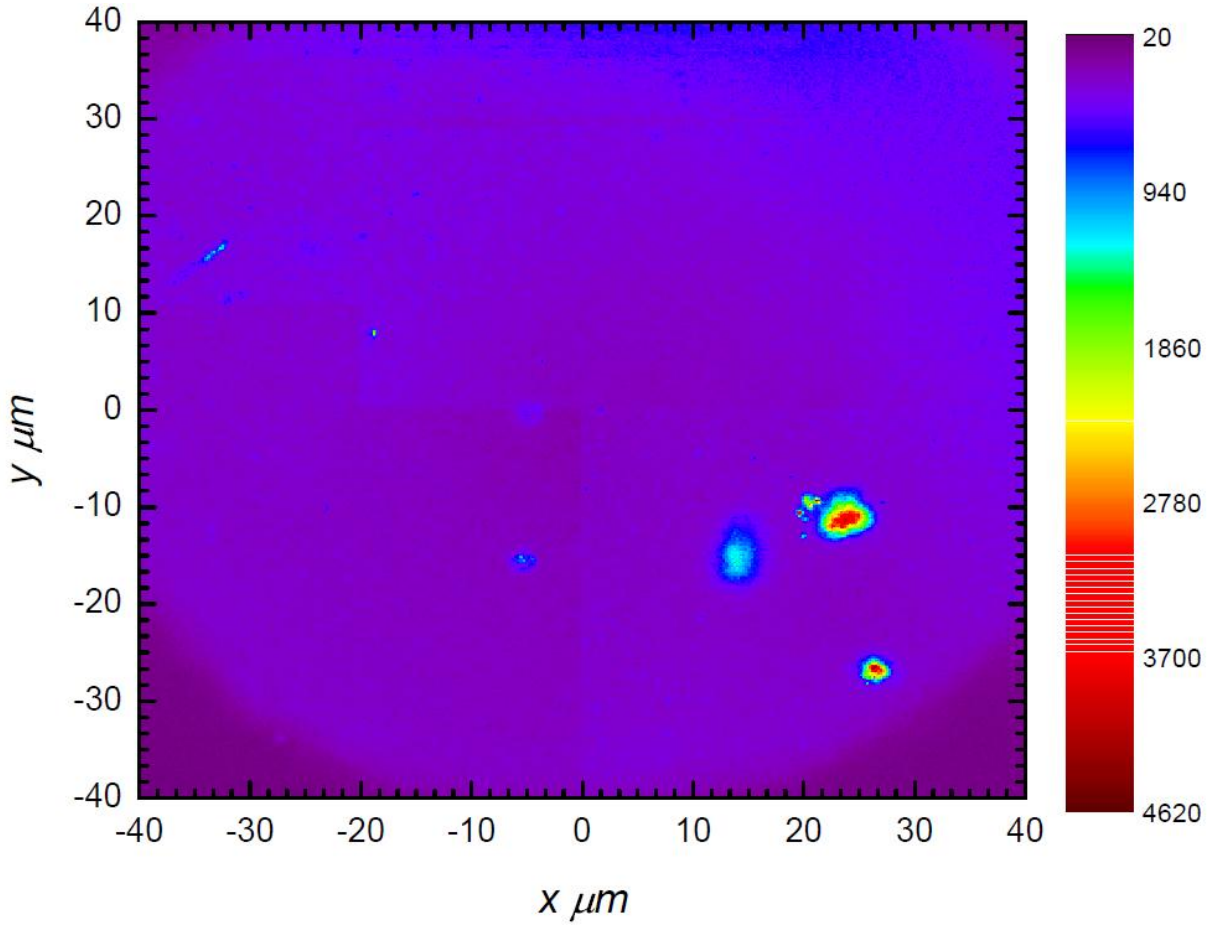

Figure 8-8 – High resolution false colour photoluminescence intensity map of a typical area of SCTF. Formed of conjoined images to give an overall resolution of 800 x 800 pixels. All the bright features observed where organic matter that rapidly photobleached if examined. Obtained with the 100x lens using 532nm excitation.

SCTF was found to contain a minimal concentration of defect centres, (see Figure 8-8). As such, SCTF was sent to Dr D. Wildanger for nitrogen ion implantation of a square array to give a square array of NV centres. The sample was annealed to allow the NV centres to form. Following annealing, cleaning was completed by aqua regia soak and boils as for ED1 and ED2. It is clear that further cleaning is required to remove surface defects as with ED1 and ED2 (see Figure 8-9). Again, depositions of graphite are observed, with the distribution found to be even across the sample. As a result, it was not possible to identify the presence of an array of defect centres.

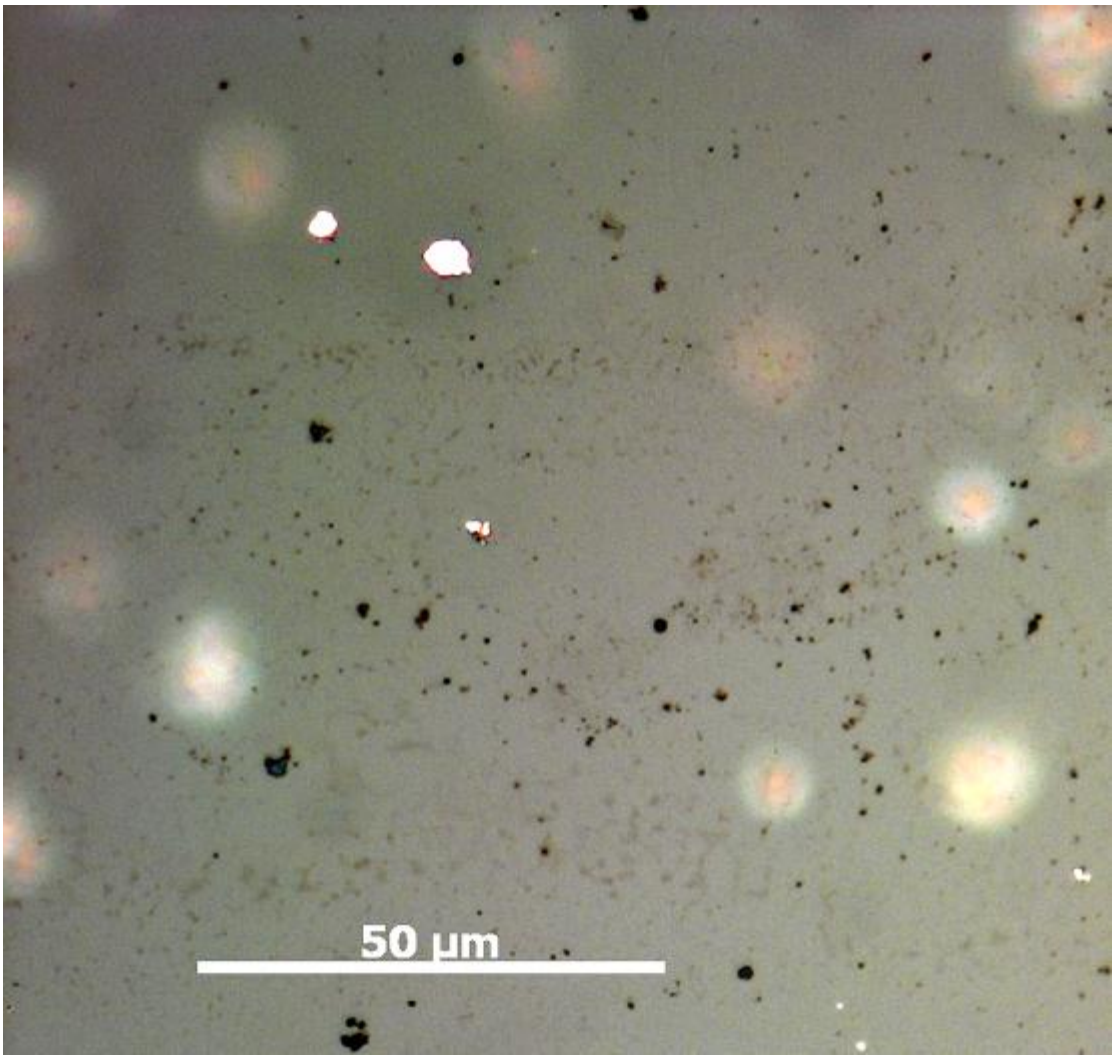

Figure 8-9 – Optical micrograph taken in reflection of surface defects on SCTF following annealing.

9 Conclusions

The results demonstrate a number of important developments in the understanding of processing and characterisation of the NV centre and other optical structures in diamond.

Success has been met in the understanding of the process occurring in diamond through the use of dual aberration corrected femtosecond laser milling. Structures have been made using this technique which have been characterised and show an improved understanding of the effects of introducing amorphous carbon to the system. It has been possible to demonstrate the damaging effect that the expansion from diamond to amorphous carbon has on the diamond and ways that this may be mitigated have been detected.

Further knowledge has been gained in the understanding of annealing of diamond, in particular the now expected presence of graphite deposits on the diamond surface following annealing. A technique to remove these has been identified and prepared.

A process that will allow for controlled removal of the graphite phase introduced in the diamond through the femtosecond laser milling has been identified, although it is reliant on the success of the cleaning phase in order to make a quantifiable measurement of its success.

The use of millimetre scale solid immersion lenses has been examined and some success has been had. Namely it has been possible to demonstrate the increase in numerical aperture expected through the use of a Weierstrass optic.

A number of samples have been characterised, the most notable of which is the presence of such a high concentration of nitrogen vacancies in the polycrystalline thin film diamond.

The development of the periscope system of the scanning confocal microscope has allowed for a number of new experiments to be performed and gives an improved system for easy exchange of experimental setups for imaging. The versatility it has indicates that it is a successful addition.

10 Further Work

There are a number of areas of this project that require further work to gain a full appreciation of the diamond systems characterised.

Although designed, the most important experiment to implement will be the cleaning of the diamond samples following annealing using a tri-acid boil. It has not been possible to obtain a number of expected results due to an inability to characterise the samples using scanning confocal microscopy following annealing.

Following on from the cleaning required, the engineering diamond samples, 1 and 2 require processing to remove the graphite structures. The experimental work has been successful in identifying a likely process to do this, using a hydrochloric acid electrochemical attack to selectively remove the graphite. In order to examine the success of this method, the cleaned diamonds will have to have a secure electrical contact made with the ends of the graphite structures. This in itself presents a number of challenges, but it is expected that these will be readily overcome.

The examination using the super solid immersion lens requires the identification of defect centres at a depth much closer to the focal plane of the lens in order to examine the light collection properties of the system and to allow the losses at the interface to be overcome.

A development of a more precise technique to position the solid immersion lenses on the surface of the diamonds would allow for a direct comparison to be made between the three lenses examined. Currently, it is has not been possible to image the same features using different lenses successfully as it is not possible to position the lens to micron-scale accuracy without moving the sample on the stage to an extent.

11 Project Management

In the first project management form, I stated the aims of this project were to:

- Design featured diamond surfaces using finite difference time domain (FDTD) modelling
- Fabricate features on silica-on-diamond using FIB milling and transfer-etched through collaboration with University of Strathclyde
- Identify isolated nitrogen vacancy centres and fabricate features around identified centres.

In this project, I have not been able to bring to fruition any of these stated aims. Whilst I have made good headway towards them, the aims have changed steadily with developments in the project. I will address each of the above points in turn.

Firstly, I have not used FDTD modelling extensively to design featured diamond surfaces. I made some progress initially and completed basic training in how to use FDTD modelling, but rapidly found the project direction shifting due to other collaborations I was involved with. The primary collaboration I have been working on was with Dr Martin Booth's group of the Department of Engineering. An earlier collaboration between Mr Philip Dolan and the stated group led to the development of the opportunity to create internal structures in diamond using laser milling. I was given the opportunity to test the new confocal microscope setup that I had developed in order to characterise a number of test structures created by this process. In doing so, I was able to identify a number of interesting and important areas of investigation that would allow this technique to be used to create optical structures, the first of which was to examine the effect of annealing.

The second aim I identified at the start of the project was to use FIB milling to create featured surfaces on diamond. This aim was hampered by a number of problems. Firstly, upon my completion of FIB training, it was a number of weeks before it was possible to book a session on the FIB to complete milling. In this initial session, and a second session, I identified that the surface structure of the sample was not uniform as the group had been told. In this sample, collaboration with the University of Strathclyde, and the group of Dr Erdan Gu, a layer of silicon was deposited on diamond

and I was to use the FIB to ablate the surface in a controlled manner to give optical structures that would then be transferred through etching to the diamond by the Strathclyde group. The effect of the surface being non-uniform made it impossible to create accurate optical structures, and the sample was returned to Strathclyde for their opinion on the matter. It was a number of months before any confirmation of our findings were received and it was not until late March that an alternative sample was offered, by which point the other areas of investigation had developed to the point that it would not be realistic to attempt further work on this area of the project.

The identification of single defect centres in diamond continued throughout the year, but I was hampered in my efforts by a number of problems that arose. Regular investigation of the diamonds led to surface contamination by air-borne particles giving large amounts of background noise in measurements. Initial cleaning attempts were not sufficient and often resulted in more noise than there had been beforehand. It took me a few months to get the "knack" of cleaning the diamonds for use. This occasionally meant that some diamonds were to be cleaned by various acid techniques. Acid cleaning was not always possible due to the requirement to use the fume hoods and expertise of other people in the department. In addition to this, during one particular period of more successful investigation, the computer running the TCPCS card – required to take Hanbury-Brown and Twiss measurements – suffered a hardware failure. It was more than six weeks before this computer was operational and measurements could be taken.

Running concurrently with the investigations above, were a number of experiments involving the engineering diamonds. In particular, the effect of annealing led to a number of unexpected problems; the primary of which was the identification of decomposition of regions of the diamond surface to graphite. This unexpected effect required significant removal in order to examine the diamonds. I made regular attempts with continually more oxidising cleaning methods to remove the contamination, but these had no effect. In order to continue, I identified that the regularly used, but hazardous technique of tri-acid boiling would likely be required. This required the design and implementation of an experiment that has not been conducted in the department to date. As such, I

have not been able to complete the work by this date owing to the complications and delay associated with the health and safety aspects of completing the experiment.

The second problem encountered with the engineering diamonds was identifying a method to selectively extract the graphite from the diamond following annealing. I completed a number of experiments that provided evidence for a suitable solution, however, conflicting reports from other individuals in the field led to initial complications. With the literature and direct contact with one group suggesting that a high current and voltage combination was required, yet a second source telling us that the process could be achieved under comparatively simple conditions. The complications of the diamond cleaning that was required following annealing have led to neither being attempted on the diamonds as yet.

Despite these complications to the progression of the project, I have remained within the broad remit of the title and have contributed useful information to the groups understanding of a number of processes. I feel that the project has been successful on the whole as a result.

PROJECT MANAGEMENT FORM 1

Part II Project Description Form

After discussion with your supervisor YOU should complete this form and send a copy to the Academic Administrator's Secretary by Friday of 0th week of Michaelmas Term.

Name: Alasdair Morrison College: Mansfield
Address for correspondence: Mansfield College, Mansfield Road, OX1 3TF

Contact telephone number: 07944932646

Title of project: Optical Structures in Diamond

Supervisor: Jason Smith

What are the objectives of the project in order of priority?

- Design of featured diamond surfaces using finite difference time domain (FDTD) modelling
- Fabricate features on silica-on-diamond using FIB milling and transfer-etched through collaboration with University of Strathclyde
- Identify isolated nitrogen vacancy centres and fabricate features around identified centres

List the major milestones that must be accomplished in order to meet the objectives of the project

- Modification of scanning confocal microscope to allow for horizontal imaging of thin film diamond samples
- Learning how to use FDTD software, development of skills
- Ensure samples transfer-etched by University of Strathclyde collaborators

Are you working essentially on your own or as part of a team? If you are part of a team what is your role, and to what extent is the success of your project dependent on other members of the team?

- Part of a team, project requires collaboration with external groups, alternative project routes available if problems arise.

What resources (equipment, materials, technician support etc.) will you need?

- Thin-film diamond and nanodiamonds provided by collaborators.

Do you require any training to meet your objectives, e.g. in the use of specific experimental equipment or software, and how are you going to obtain that training?

- Basic training in FDTD software - obtained
- Training in use of FIB - planned

Complete the following plan for your entire project as you see it now. List each major task down the left hand column, and for each one draw a horizontal line to indicate the period you expect to allocate to it. For example, the final task, writing your thesis, is shown as occupying mid-April to mid-June.

Task	Oct	Nov	Dec	Jan	Feb	Mar	Apr	May	Jun
Modification of scanning confocal microscope	--								
Design of structures using FDTD	------	------	------	------					
FIB Training	---								
Fabrication of structures in silicon-on-diamond	---	------	------	------	-----				
Characterisation of thin film diamonds and structures	------	------	------	------	------	------	-----		
Initial Literature review	------	------							
Writing up							xxxx	xxxx	xxxx

Has your supervisor completed a *Risk Assessment Form* about your project yet?

Your signature: Your supervisor's signature:
Date: Date:

PROJECT MANAGEMENT FORM 2

1st Part II Project Analysis Form

Complete this form and send a copy to the Academic Administrator's Secretary by Friday of 6th week of Michaelmas Term

Name: Alasdair Morrison
Title of Project as given in your Project Description: Optical Structures in Diamond

Refer back to the project plan in your Project Description and list the goals you set for this term. Comment briefly on the extent to which you have achieved them.

- Design of featured diamond surfaces using finite difference time domain (FDTD) modelling – on-going, working to schedule.
- Fabricate features on silica-on-diamond using FIB milling and transfer-etched through collaboration with University of Strathclyde – investigation as to the extent of suitable material for milling completed. Features due for fabrication when FIB available.
- Identify isolated nitrogen vacancy centres and fabricate features around identified centres – identification under way on a number of samples, determining method to precisely mark location for future reference

Identify clearly any difficulties you have encountered. Are they surmountable in the time available?

- FIB 200 source problems have prevented its use. Examining other samples that do not require milling immediately and progressing on a parallel path where FIB is not required.

State any refinements, modifications or replacements of the original objectives for your Part II project:

- Characterise the results of focused laser milling to create optical structures in diamond. Identify method to selectively etch the damaged diamond and characterise results.

Are you intending to change the title of your project? If so, state the new title: N/A

Have the training needs you identified in the Project Description been met, and have you identified any further training requirements?
Training requirements met. No further training currently required.

Tick the appropriate box. Do you have

	None	Some	Sufficient
Results		x	
Analysis of results		x	

Do you have any other comments you wish to make? None.

After looking at the project plan in your Project Description complete the following project plan for the remainder of your Part II.

Task	Dec	Jan	Feb	Mar	Apr	May	Jun
Design of structures using FDTD	------	------	------				
Investigation of focused laser milling	---						
Fabrication of structures in silicon-on-diamond	--------	--------	--------	--------			
Characterisation of thin film diamonds and structures	--------	--------	--------	--------	--------	--------	
Initial Literature review	--------						
Writing up					xxxxx	xxxxx	xxxxx

General comments by the supervisor:

Your signature:
Date:

Your supervisor's signature:
Date:

PROJECT MANAGEMENT FORM 3

2nd Part II Project Analysis Form

Complete this form and send a copy to the Academic Administrator's Secretary by Friday of 6th week of Hilary Term

Name: Alasdair Morrison

Title of Project: Optical Structures in Diamond

Refer back to the project plan you made last term and list the goals you set for this term. Comment briefly on the extent to which you have achieved them.

- Design of featured diamond surfaces using finite difference time domain (FDTD) modelling. Some under way but less relevant.
- Fabricate features on silica-on-diamond using FIB milling and transfer-etched through collaboration with University of Strathclyde – investigation as to the extent of suitable material for milling completed. Sample issues have prevented this from occurring.
- Identify isolated nitrogen vacancy centres and fabricate features around identified centres – identification under way on a number of samples, progress made and good results obtained.

Identify clearly any difficulties you have encountered. Are they surmountable in the time available?

- Difficulty in identification of a possible etching technique for graphite in diamond samples to remove graphite. Possible solutions being investigated. Should be surmountable.

State any refinements, modifications or replacements of the objectives you set for your Part II project:

- Design of structures in line with existing work in the field using focused laser milling to mill features, followed by etching and characterisation.

Are you intending to change the title of your project? If so, state the new title:
No

What is the title of the talk you will give to the Department?
Optical Structures in Diamond

Have all your training needs for this project now been met?
Yes

Tick the appropriate box. Do you have

	None	Some	Sufficient
Results		Yes	
Analysis of results		Yes	

Do you have any other comments you wish to make?

General comments by the supervisor:

Your signature:
Date:

Your supervisor's signature:
Date:

12 Bibliography

[1] J. F. Prins, “Diamond,” in *Encylopedia of Materials2001: Science and Technology (second edition)*, Oxford, Elsevier, 2001, pp. 2108-2112.

[2] D. F. Edwards and E. Ochoa, “Infrared Refractive-Index of Diamonds,” *Journal of the Optical Soceity of America,* vol. 71, no. 5, pp. 607-608, 1981.

[3] F. Jelezko and J. Wrachtrup, “Single defect centres in diamond: A review,” *Physica Status Solidi (A),* vol. 203, no. 13, pp. 3207-3225, 2006.

[4] J. M. Smith, F. Grazioso, B. R. Patton, P. R. Dolan, M. L. Markham and D. J. Twitchen, “Optical properties of a single-colour centre in diamond with a green zero-phonon line,” *New Journal of Physics,* vol. 13, p. 045005, 2011.

[5] C. D. Clark and C. A. Norris, “Photoluminescence Associated with 1.673, 1.944 and 2.498 Ev Centres in Diamond,” *Journal of Physics Part C Solid State Physics,* vol. 4, no. 14, pp. 2223-2229, 1971.

[6] L. du Preez, “PhD Thesis,” University of Witwatersrand, Witwatersrand, 1965.

[7] G. Davies and M. F. Hamer, “Optical studies of the 1.945eV vibronic band in diamond,” *Proceedings of the Royal Society of London.A. Mathematical and Physical Sciences,* vol. 348, no. 1653, pp. 285-298, 1976.

[8] E. Oort, N. Manson and M. Glasbeek, “Optically detected spin coherence of the diamond NV centre in its triplet ground state,” *Journal of Physics C: Solid State Physics,* vol. 21, pp. 4385-4391, 1988.

[9] N. Manson, X. He and P. Fisk, “Raman Heterodyne Detected Electron-Nuclear-Double-Resonance Measurements of the Nitrogen-Vacancy Center in Diamond,” *Optics Letters,* vol. 15, no. 19, pp. 1094-1096, 1990.

[10] I. Hiromitsu, J. Westra and M. Glasbeek, “Cross-Relaxation Dynamics of the N-V Center in Diamond as Studied Via Optically Detected Microwave Recovery Transients,” *Physical Review B,* vol. 46, no. 17, pp. 10600-10612, 1992.

[11] K. Holliday, N. Manson, M. Glasbeek and E. Oort, “Optical hole-bleaching by level anti-crossing and cross relaxation in the NV centre in diamond,” *Journal of Physics: Condensed Matter,* vol. 1, pp. 7093-7102, 1989.

[12] D. Redman, S. Brown and S. Rand, “Origin of persistent hole burning of N–V centers in diamond,” *Journal of the Optical Soceity of America,* vol. 9, no. 5, pp. 768-774, 1991.

[13] A. Lenef and S. Rand, “Electronic structure of the N-V center in diamond: Theory,” *Physical Review B,* vol. 53, no. 20, pp. 13441-13455, 1996.

[14] A. Lenef, S. Brown, D. Redman, S. Rand, J. Shigley and E. Fritsch, “Electronic structure of the N-V center in diamond: Experiments,” *Physical Review B,* vol. 53, no. 20, pp. 13427-13440, 1996.

[15] F. Jelezko, T. Gaebel, I. Popa, A. Gruber and J. Wrachtrup, “Observation of coherent oscillations in a single electron spin,” *Physical Review Letters,* vol. 92, no. 7, p. 764041, 2004.

[16] P. Neumann, N. Mizuochi, F. Rempp, P. Hemmer, H. Watanabe, S. Yamasaki, V. Jacques, T. Gaebel, F. Jelezko and J. Wrachtrup, “Multipartite entanglement among single spins in diamond,” *Science,* vol. 320, no. 5881, pp. 1326-1329, 2008.

[17] R. Hanson, O. Gywat and D. Awschalom, “Room-temperature manipulation and decoherence of a single spin in diamond,” *Physical Review B,* vol. 74, no. 16, p. 161203, 2006.

[18] N. Manson, J. Harrison and M. Sellars, “Nitrogen-vacancy center in diamond: Model of the electronic structure and associated dynamics,” *Physical Review B,* vol. 74, no. 10, p. 104303, 2006.

[19] J. Larsson and P. Delaney, “Electronic structure of the nitrogen-vacancy center in diamond from first-principles theory,” *Physical Review B,* vol. 77, no. 16, p. 165201, 2008.

[20] A. Gali, M. Fyta and E. Kaxiras, “Ab initio supercell calculations on nitrogen-vacancy center in diamond: Electronic structure and hyperfine tensors,” *Physical Review B,* vol. 77, no. 15, p. 155206, 2008.

[21] M. Doherty, N. Manson, P. Delaney and L. Hollenberg, “The negatively charged nitrogen-vacancy centre in diamond: the electronic solution,” *New Journal of Physics,* vol. 13, p. 025019, 2011.

[22] A. Gruber, A. Dräbenstedt, C. Tietz, L. Fleury, J. Wrachtrup and C. Borczyskowski, “Scanning confocal optical microscopy and magnetic resonance on single defect centers,” *Science,* vol. 276, no. 5321, p. 2012, 1997.

[23] C. Kurtsiefer, S. Mayer, P. Zarda and H. Weinfurter, “Stable solid-state source of single photons,” *Physical Review Letters,* vol. 85, no. 2, pp. 290-293, 2000.

[24] W. F. Banholzer, “Diamond: Isotropically Modified,” in *Encyclopedia of Materials: Science and Technology (Second Edition)*, K. H. J. Buschow, Ed., Oxford, Elsevier, 2001, pp. 2122-2126.

[25] J. Isberg, J. Hammersberg, E. Johansson, T. Wikstrom, D. Twitchen, A. Whitehead, S. Coe and G. Scarsbrook, “High carrier mobilitiy in single-crystal plasma-deposited diamond,” *Science,* vol. 297, no. 5587, pp. 1670-1672, 2002.

[26] S. Pezzagna, D. Wildanger, P. Mazarov, A. D. Wieck, Y. Sarov, I. Rangeow, B. Naydenov, F. Jelezko, S. W. Hell and J. Meijer, “Nanoscale Engineering and Optical Addressing of Single Spins in Diamond,” *SMALL,* vol. 6, no. 19, pp. 2117-2121, 2010.

[27] J. Orwa, C. Santori, K. Fu, B. Gibson, D. Simpson, I. Aharonovich, A. Stacey, A. Cimmino, P. Balog, M. Markham, D. Twitchen, A. Greentree, R. Beausoleil and S. Prawer, “Engineering of nitrogen-vacancy color centers in high purity diamond by ion implantation and annealing,” *Journal of Applied Physics,* vol. 109, no. 8, pp. 083530.1-083530.7, 2011.

[28] I. Aharonovich and S. Prawer, “Fabrication strategies for diamond based ultra bright single photon sources,” *Diamond and Related Materials,* vol. 19, no. 7-9, pp. 729-733, 2010.

[29] S. M. Mansfield and G. S. Kino, “Solid Immersion Microscope,” *Applied Physics Letters,* vol. 57, no. 24, pp. 2615-2616, 1990.

[30] K. Serrels, E. Ramsay, P. Dalgarno, B. Gerardot, J. O'Connor, R. Hadfield, R. Warburton and D. Reid, “Solid immersion lens applications for nanophotonic devices,” *Journal of Nanophotonic,* vol. 2, no. 1, p. 021854, 2008.

[31] E. W. A. B. B. Max Born, Principles of Optics: Electromagnetic Theory of Propagation, Interference and Diffraction of Light; 7th Edition, Cambridge: Cambridge University press, 1999.

[32] W. Barnes, G. Bjork, J. Gerard, P. Jonsson, J. Wasey, P. Worthing and V. Zwiller, “Solid-state single photon sources: light collection strategies,” *European Physical Journal D,* vol. 18, no. 2, pp. 197-210, 2002.

[33] V. Zwiller and G. Björk, “Improved light extraction from emitters in high refractive index materials using solid immersion lenses,” *Journal of Applied Physics,* vol. 92, pp. 660-665, 2002.

[34] J. Hadden, J. Harrison, A. Stanley-Clarke, L. Marseglia, Y.-L. Ho, B. Patton, J. O'Brien and J. Rarity, “Strongly enhanced photon collection from diamond defect centers under microfabricated integrated solid immersion lenses,” *Applied Physics Letters,* vol. 97, no. 24, p. 241901, 2010.

[35] L. Marseglia, J. Hadden, A. Stanley-Clarke, J. Harrison, B. Patton, Y.-L. Ho, B. Naydenov, F. Jelezko, J. Meijer, P. Dolan, J. Smith, J. Rarity and J. O'Brien, “Nanofabricated solid immersion lenses registered to single emitters in diamond,” *Applied Physics Letters,* vol. 98, no. 13, p. 133107, 2011.

[36] S. Castelletto, J. Harrison, L. Marseglia, A. Stanley-Clarke, B. Gibson, B. Fairchild, J. Hadden, Y.-L. D. Ho, M. Hiscocks, K. Ganesan, S. Huntington, F. Ladouceur, A. Greentree, S. Prawer, J. O'Brien and J. Rarity, “Diamond-based structures to collect and guide light,” *New Journal of Physics,* vol. 13, p. 02502, 2011.

[37] P. Siyushev, F. Kaiser, V. Jacques, I. Gerhardt, S. Bischof, H. Fedder, J. Dodson, M. Markham, D. Twitchen, F. Jelezko and J. Wrachtrup, “Monolithic diamond optics for single photon detection,” *Applied Physics Letters,* vol. 97, no. 24, p. 241902, 2010.

[38] P. Olivero, S. Rubanov, P. Reichart, B. Gibson, S. Huntington, J. Rabeau, A. Greentree, J. Salzman, D. Moore, D. Jamieson and S. Prawer, "Ion-Beam-Assisted Lift-Off Technique for Three-Dimensional Micromachining of Freestanding Single-Crystal Diamond," *Advanced Materials,* vol. 17, no. 20, pp. 2427-2430, 2005.

[39] Y. Zhang, L. McKnight, Z. Tian, S. Calvez, E. Gu and M. D. Dawson, "Large cross-section edge-coupled diamond waveguides," *Diamond and Related Materials,* vol. 20, no. 4, pp. 564-567, 2011.

[40] M. Hiscocks, K. Ganesan, B. Gibson, S. Huntington, F. Ladouceur and S. Prawer, "Diamond waveguides fabricated by reactive ion etching," *Optics express,* vol. 16, no. 24, pp. 19512-19519, 2008.

[41] K.-M. Fu, C. Santori, P. E. Barclay, I. Aharonovich and S. Prawer, "Coupling of nitrogen-vacancy centers in diamond to a GaP waveguide," *Applied Physics Letters,* vol. 93, no. 23, p. 234107, 2008.

[42] K. Vahala, "Optical Microcavities," *Nature,* vol. 424, no. 6950, pp. 839-846, 2003.

[43] Y.-C. Liu, Y.-F. Xiao, B.-B. Li, X.-F. Jiang, Y. Li and Q. Gong, "Coupling of a single diamond nanocrystal to a whispering-gallery microcavity: Photon transport benefitting from Rayleigh scattering," *Physical Review A,* vol. 84, no. 1, p. 011805, 2011.

[44] J. Wolters, A. W. Schell, G. Kewes, N. Nuesse, M. Schoengen, H. Doescher, T. Hannappel, B. Loechel, M. Barth and O. Benson, "Enhancement of the zero phonon line emission from a single nitrogen vacancy center in a nanodiamond via coupling to a photonic crystal cavity," *Applied Physics Letters,* vol. 97, no. 14, p. 141108, 2010.

[45] C. Kreuzer, J. Riedrich-Möller, E. Neu and C. Becher, "Design of photonic crystal microcavities in diamond films," *Optics Express,* vol. 16, no. 3, pp. 1632-1644, 2008.

[46] J. Riedrich-Moeller, L. Kipfstuhl, C. Hepp, E. Neu, C. Pauly, F. Muecklich, A. Baur, M. Wandt, S. Wolff, M. Fischer, S. Gsell, M. Schreck and C. Becher, "One- and two-dimensional photonic

crystal microcavities in single crystal diamond," *Nature Nanotechnology,* vol. 7, no. 1, pp. 69-74, 2012.

[47] A. Faraon, P. E. Barclay, C. Santori, K.-M. C. Fu and R. G. Beausoleil, "Resonant enhancement of the zero-phonon emission from a colour centre in a diamond cavity," *Nature Photonics,* vol. 5, no. 5, pp. 301-305, 2011.

[48] B. Hausmann, B. Shields, Q. Quan, P. Maletinsky, M. McCutcheon, J. Choy, T. Babinec, A. Kubanek, A. Yacoby and M. Lukin, "Integrated diamond networks for quantum nanophotonics," *Nano Letters,* 2011.

[49] T. Babinec, B. Hausmann, M. Khan, Y. Zhang, J. Maze, P. Hemmer and M. Lončar, "A diamond nanowire single-photon source," *Nature nanotechnology,* vol. 5, no. 3, pp. 195-199, 2010.

[50] I. Villalpando, P. John, S. Porro and J. Wilson, "Hydrogen plasma etching of diamond films deposited on graphite," *Diamond and Related Materials,* vol. 20, no. 5-6, pp. 711-716, 2011.

[51] M. Takesada, E. Vanagas, D. Tuzhilin, I. Kudryashov, S. Suruga, H. Murakami, N. Sarukura, K. Matsuda, S. Mononobe and T. Saiki, "Micro-character printing on a diamond plate by femtosecond infrared optical pulses," *Japanese journal of applied physics,* vol. 42, no. Part 1, pp. 4613-4616, 2003.

[52] T. Kononenko, M. Komlenok, V. Pashinin, S. Pimenov, V. Konov, M. Neff, V. Romano and W. Lüthy, "Femtosecond laser microstructuring in the bulk of diamond," *Diamond and Related Materials,* vol. 18, no. 2-3, pp. 196-199, 2009.

[53] R. Simmonds, T. Wilson and M. Booth, "Effects of aberrations and specimen structure in conventional, confocal and two-photon fluorescence microscopy," *Journal of Microscopy,* vol. 245, no. 1, pp. 63-71, 2012.

[54] R. Simmonds, P. Salter, A. Jesacher and M. Booth, "Three dimensional laser microfabrication in diamond using a dual adaptive optics system," *Optics Express,* vol. 19, no. 24, pp. 24122-241228, 2011.

[55] N. Y. Stozhko, N. A. Malakhova, M. V. Fyodorov and K. Z. Brainina, “Modified carbon-containing electrodes in stripping voltammetry of metals. Part II. Composite and microelectrodes,” *Journal of Solid State Electrochemistry,* vol. 12, no. 10, pp. 1219-1230, 2008.

[56] D. Andrew L., “The role of carbon in fuel cells,” *Journal of Power sources,* vol. 156, no. 2, pp. 128-141, 2006.

[57] F. Cocks and H. LaViers, “Carbon-ion fuel cell for the flameless oxidation of coal”. United States of America 1994.

[58] N. Cherepy, R. Krueger, K. Fiet, A. Jankowski and J. Cooper, “Direct conversion of carbon fuels in a molten carbonate fuel cel,” *Journal of the Electrochemical Society,* vol. 152, p. A80, 2005.

[59] M. M., “Diamond: Natural,” in *Encyclopedia of Materials: Science and Technology (Second Edition)*, Oxford, Elsevier, 2001, pp. 2133-2143.

[60] M. B., “Carbons and Graphites, Mechanical Properties of,” in *Encyclopedia of Materials: Science and Technology (Second Edition)*, Oxford, Elsevier, 2001, pp. 967-975.

[61] P. Hapiot and C. Lagrost, “Electrochemical reactivity in room-temperature ionic liquids,” *Chemical reviews,* vol. 108, no. 7, pp. 2238-2264, 2008.

[62] M. Galinski, A. Lewandowski and I. Stepniak, “Ionic liquids as electrolytes,” *Electrochimica Acta,* vol. 51, no. 26, pp. 5567-5580, 2006.

[63] J. Wrachtrup and F. Jelezko, “Processing quantum information in diamond,” *Journal of Physics-Condensed Matter,* vol. 18, no. 21, pp. S807-S824, 2006.

[64] C. Santori, P. Barclay, K. Fu, R. Beausoleil, S. Spillane and M. Fisch, “Nanophotonics for quantum optics using nitrogen-vacancy centers in diamond,” *Nanotechnology,* vol. 21, p. 274008, 2010.

[65] P. E. Barclay, K.-M. C. Fu, C. Santori and R. G. Beausoleil, “Chip-based microcavities coupled to nitrogen-vacancy centers in single crystal diamond,” *Applied Physics Letters,* vol. 95, no. 19, p. 191115, 2009.

[66] J. L. O'Brien, “Optical quantum computing,” *Science,* vol. 318, no. 5856, pp. 1567-1570, 2007.

[67] A. Beveratos, R. Brouri, T. Gacoin, A. Villing, J. Poizat and P. Grangier, “Single photon quantum cryptography,” *Physical Review Letters,* vol. 89, no. 18, p. 187901, 2002.

[68] H. Kimble, “The quantum internet,” *Nature,* vol. 453, no. 7198, pp. 1023-1030, 2008.

[69] I. Aharonovich, A. Greentree and S. Prawer, “Diamond Photonics,” *Nature Photonics,* vol. 5, no. 7, pp. 397-405, 2011.

[70] F. Grazioso, B. Patton and J. Smith, “A high stability beam-scanning confocal optical microscope for low temperature operation,” *Review of Scientific Instruments,* vol. 81, p. 093705, 2010.

[71] K. Mann, G. Pfeifer and G. Reisse, “Damage threshold measurements using femtosecond excimer laser,” in *SPIE*, 1993.

[72] J. C. Scully, The Fundamentals of Corrosion, second edition, Oxford: Pergamon, 1975.

[73] K. R. Tretheway and J. Chamberlain, Corrosion, For students of science and engineering, Harlow: Longman Scientific and Technical, 1988.

[74] J. R. Davis, Corrosion, Understanding the Basics, Materials Park, Ohio, USA: ASM International, 2008.

[75] E. Hecht, Optics, third edition, Addison Wesley Longman, 1998.

[76] M. Fox, Quantum Optics; An Introduction, Oxford: Oxford University Press, 2006.